

**THERMAL TRANSFORMATION OF PERFLUOROOCCTANESULFONIC
ACID (PFOS) AND PERFLUOROOCCTANOIC ACID (PFOA) IN SPIKED
SAND: IDENTIFICATION OF NOVEL PRODUCTS OF INCOMPLETE
DEGRADATION**

by

Samer Al-Dirani

A thesis submitted to the Department of Civil Engineering

In conformity with the requirements for
the degree of Master of Applied Science

Queen's University

Kingston, Ontario, Canada

(November 2022)

Copyright ©Samer Al-Dirani, 2022

Abstract

This study explored thermal conductive heating (250 °C to 550 °C) in the presence of air for remediating silica sand spiked with perfluorooctanoic acid (PFOA) and perfluorooctanesulfonic acid (PFOS) at 50 and 200 mg PFAS/kg sand. The fate of PFAS and fluorine was quantified with sand and emission analysis, including targeted PFAS, transformation products, and soluble fluorine. Post-treatment PFAS sand concentrations at temperatures above 400 °C were below detection limits (0.0004 mg/kg), with >99% removal efficiency. However, at 300 °C and 250 °C, PFOA and PFOS remained above regulatory guidelines. TFA and PFPA were the most detected PFAS in emissions at temperatures >400 °C, whereas PFHpA, PFHxA, and PFPeA were the main emissions at 300 °C and 250°C. Long-chain PFAS (>C9) were identified in the emission system at all temperatures indicating that PFAS radicals can combine to form long-chain PFAS. Several novel PFAS transformation products, including 4,5,6,6,7,7,8,8,8-nonafluorooct-2,4-enoic acid and 2,3,4,5,6,6,7,7,8,8,8-undecafluorooct-2,4-enoic acid, and homologous series of perfluoroalkyl amides (C₈HONF₁₅) were detected during high-resolution analysis of the emissions. The finding from this study proves the wide presence of PFAS in emissions during thermal treatment processes and that some of these compounds are not fully understood in terms of their physiochemical or toxicological characteristics.

Acknowledgments

I want to thank my fellow graduate students for their kindness and support throughout my time in the Civil Engineering department. Thank you to the technicians and support staff in Ellis, Michell Hall, and Royal Military College; I would have been lost without your instruction. Finally, thank you to Dr. Kueper, Dr. Weber, and David Patch, whose guidance, patience, and support have made my graduate experience genuinely positive. Funding for this research was provided by the Natural Sciences and Engineering Research Council (NSERC) of Canada through Collaborative Research and Development Grant CRDPJ 530133-18 in partnership with Imperial Oil and Golder Associates.

Table of Contents

Abstract	ii
Acknowledgments.....	iii
Chapter 1	1
Introduction.....	1
1.1 PFAS Thermal Remediation Challenges	1
1.2 Research Objectives.....	2
1.3 Thesis Outline	3
Chapter 2.....	4
Literature Review.....	4
2.1 PFAS Diversity	4
2.2 Sources of PFAS in Soil	6
2.2.1 Firefighting Foams	7
2.2.2 Wastewater	8
2.2.3 Landfill Leachate.....	8
2.3 Short-chain PFAS and Precursor Transformation	9
2.4 Biological Effect of PFAS Exposure	10
2.5 Environmental Behavior of PFAS in Soil.....	11
2.5.1 Properties Affecting PFAS Sorption and Desorption Behavior	12
2.6 PFAS Remediation Strategies.....	14
2.7 Non-destructive Remediation of PFAS-contaminated media.....	15
2.7.1 Immobilization/Sorption.....	15
2.7.2 Phytoremediation.....	18

2.7.3	Excavation and Specialized Landfills and Encapsulation	19
2.7.4	Groundwater Pump and Treat.....	20
2.7.5	Soil Flushing.....	21
2.7.6	Soil Washing.....	22
2.8	Destructive Methods for PFAS Removal from Soil	23
2.8.1	Bioremediation	23
2.8.2	In-situ Chemical Oxidation	24
2.8.3	Degradation of PFAS via Controlled Irradiation.....	25
2.8.4	Ball Milling.....	25
2.8.5	Vitrification	27
2.8.6	Pyrolysis and Gasification	28
2.8.7	Smoldering Combustion.....	29
2.8.8	Hydrothermal Liquefaction	30
2.9	Thermal Destructive Technologies	30
2.9.1	In Situ Thermal Treatment Technologies (ISTT).....	30
2.9.2	In Situ Thermal Technologies for Destroying PFAS	30
Chapter 3.....		33
Laboratory and Modelling Study Evaluating Thermal Remediation of PFOA- and PFOS-		
impacted Sand.....		33
3.1	Background.....	33
3.2	Delimitations.....	34
3.3	Material and Methods	35
3.3.1	PFAS Spiked Sand Preparation	35

3.3.2	Heating Cylinder Apparatus	35
3.3.3	PFAS Emission Collection System	36
3.4	Experimental Analysis	38
3.4.1	PFAS Targeted Analysis	38
3.4.2	PFAS Suspect Screening Analysis	38
3.4.3	Soluble Fluoride Analysis	38
3.5	Results and Discussion	39
3.5.1	Experimental Phases	39
3.5.2.1	<i>Phase I: Post-treatment Sand Analysis</i>	39
3.5.3	PFAS GAC Breakthrough and Distribution in the Impingers	44
3.5.4	PFAS Distribution in Different Heat Sinks	45
3.5.5	PFAS Emission Analysis at Different Treatment Temperatures	46
3.5.6	PFAS Transformation Products at 550°C	48
3.5.6.1	<i>Products of Incomplete Degradation</i>	49
3.5.6.2	<i>Perfluoroalkyl Amides (PFAAs)</i>	51
3.6	Summary of PFAS Recovered and Proposed Degradation and Transformation Pathways	54
3.7	Environmental Significance	55
	Chapter 4	57
4.1	Conclusions	57
4.2	Recommendations	59
	Literature Cited	61
	Appendices	71
	Appendix A: Pictures of the Laboratory Setup	71

Appendix B: PFAS Cylinder Setup and Temperature Profiles	74
Appendix C: PFAS Analysis Procedure.....	77
C.1 Solid Sample Extraction	77
C.2 PFAS Targeted Analysis	77
C.3 PFAS Suspect Screening Analysis	79
C.4 Fluoride ion-selective electrode (ISE).....	79
Appendix D: Quality Control and Quality Assurance Guidelines	81
Appendix E: Experimental Cleaning Procedure	82
Appendix F: PFOA and PFOS Pre- and Post-treatment Concentrations	83
Appendix G: Mass of Fluorine Recovered from Each Experiment	84
Appendix H: Mass of Individual PFAS captured by the Emissions	85
Appendix I: List of Known PFAS Detected in the First sorption Tubes at 550°C.....	86
Appendix J: Orbitrap Experimental Setup	87
Appendix K: Chromatogram Images for First Sorption Tube at 550°C.....	89
Appendix L: List of Unknown PFAS Detected in the First sorption Tubes at 550°C	90

List of Figures

FIGURE 1 (A) PICTURE OF THE SETUP SHOWING TO THE RIGHT THE CYLINDER HOLDING THE PFAS-CONTAMINATED SAND INSIDE THE OVEN AND TO THE LEFT THE GAS CAPTURE SYSTEM. (B) SCHEMATIC REPRESENTATION OF THE HEATING AND EMISSION COLLECTION SYSTEM (FROM RIGHT TO LEFT).	37
FIGURE 2: (A) PRE-AND POST-TREATMENT PFAS ₁₈ CONCENTRATIONS FOR PFOS AND PFOA CONTAMINATED SAND (B.D.L =0.0002 MG/KG). (B) FLUORINE MASS BALANCE ON POST-TREATMENT EXPERIMENTS WITH SPIKED PRE-TREATMENT SAND ADJUSTED BY THE 95% OF EMISSIONS THAT WERE ESCAPED BY THE FUME HOOD. POST-TREATMENT PFAS ₁₈ IN THE SOIL IS PLOTTED FOR ALL TEMPERATURES BUT IS TOO SMALL TO BE VISIBLE.	40
FIGURE 3: (A) PRE-AND POST-TREATMENT PFAS ₁₈ CONCENTRATIONS FOR PFOS- AND PFOA CONTAMINATED SAND (B.D.L =0.0002 MG/KG) AT 250 °C AND 300°C (B) FLUORINE MASS BALANCE ON POST-TREATMENT EXPERIMENTS WITH SPIKED PRE-TREATMENT SAND.	42
FIGURE 4: PERCENTAGE OF PFAS CAPTURED BY THE XAD VS. IMPINGER IN THE EMISSION LINE	44
FIGURE 5: PFAS RECOVERED AFTER THERMAL TREATMENT AT 550 °C, 500 °C, AND 400 °C FOR 75 MINUTES IN DIFFERENT RECOVERY SINKS.	45
FIGURE 6: (A) MASS (UG) OF ULTRA-SHORT CHAIN, SHORT-CHAIN, MEDIUM-CHAIN, AND LONG-CHAIN PFAS CAPTURED BY EMISSION. (B) MASS (UG) OF INDIVIDUAL PFAS CAPTURED BY THE EMISSIONS. LONG-CHAIN PFAS ARE PLOTTED FOR ALL TEMPERATURES BUT ARE TOO SMALL TO BE VISIBLE....	46
FIGURE 7: SCHEMATIC REPRESENTATION SHOWING THE TRANSFORMATION OF PFOA AND PFOS ON THE SAND MATRIX AND EMISSIONS.	48
FIGURE 8: FULL SCAN BASE PEAK MS CHROMATOGRAM OF THE METHANOL EXTRACT OF XAD-1 AT 550 °C SHOWING THE PRESENCE OF (A) PFHxDA, (B) 4,5,6,6,7,7,8,8,8-NONAFLUOROOCCT-2,4-ENOIC ACID, AND (C) 2,3,4,5,6,6,7,7,8,8,8-UNDECAFLUOROOCCT-2,4-ENOIC ACID.	50
FIGURE 9: (A) FULL SCAN BASE PEAK MS CHROMATOGRAM OF THE METHANOL EXTRACT OF XAD-1 AT 550 °C SHOWS THE PEAK'S INTENSITY AT 6.52 MINUTES AFTER REMOVING THE BACKGROUND NOISE. (B) COMPLETE SCAN BASE PEAK MS CHROMATOGRAM OF THE METHANOL EXTRACT OF XAD-1 AT 550 °C, SHOWING THE RELATIVE ABUNDANCE OF A PERFLUOROALKYL AMIDE (C ₈ HONF ₁₅) AT 6.52 MINUTES.	51
FIGURE 10: FULL-SCAN BASE PEAK MS CHROMATOGRAM OF THE METHANOL EXTRACT OF XAD-1 AT 550 °C SHOWINGS: (A) C ₈ TO C ₃ AMIDES WITH THEIR CORRESPONDING INTENSITIES, (B) C ₈ TO C ₁₇ AMIDES WITH THEIR CORRESPONDING INTENSITIES.	53
FIGURE 11: PFAS DETECTED IN THE FIRST SORPTION TUBE AT 550°C WITH SOME OF THEIR PROPOSED MECHANISMS.	54

List of Tables

TABLE 1: PHYSICAL AND CHEMICAL PROPERTIES OF PFOA AND PFOS [19]	4
TABLE 2: THE MOST STUDIED PFAS IN THE LITERATURE [23]	5
TABLE 3: SUMMARY STATISTICS FOR PFOA AND PFOS MEASURED BY MATRIX [24]	7
TABLE 4: RELEVANT BOND ENERGIES FOR SOME FLUORINATED COMPOUNDS	33

Chapter 1

Introduction

1.1 PFAS Thermal Remediation Challenges

Per- and polyfluoroalkyl substances (PFAS) have been used extensively since the 1950s in commercial, industrial, and military applications due to their dual hydrophobic/hydrophilic surface-active properties and chemical/thermal stability [1]. The widespread use and adaptability of PFAS have resulted in contamination of groundwater, surface water, drinking water, and soil [2] [3] [4]. Perfluorooctanoic acid (PFOA) and perfluorooctanesulfonic acid (PFOS) are two of the most detected long-chain PFAS in contaminated field soil [5]. Many governmental environmental agencies have classified PFOA and PFOS as emerging contaminants, including the United States Environmental Protection Agency (USEPA) [6]. The recent adoption of regulatory limits concerning the use of PFAS has created intense interest in developing remediation options for water and soil [7] [8]

Existing soil remediation technologies have been proven ineffective for PFAS contamination [9] [10]. The wide variety of PFAS present at any given site creates challenges since most technologies cannot break down all types of PFAS. In addition, the strong carbon-fluorine bonds of PFAS make them highly recalcitrant and resistant to destruction [11].

Thermal remediation is a viable remediation strategy for most organic contaminants, such as chlorinated solvents, coal tar, and crude oil. Heat increases the vapour pressure of organic compounds and increases partitioning to the gas phase to enhance vapor recovery. One of the main

advantages of thermal treatment is that up to 99% of the substrates can be treated regardless of the contaminant chemical species [12] [13].

One challenge in using in-situ thermal technologies is the need for proper site characterization, specifically accurate conceptual site models [14]. Poor site characterization before thermal treatment can cause the volatile contaminants to travel to other areas. Recent incineration studies have shown that in-situ thermal treatment of PFAS-contaminated soil in an oven between 400 °C to 500 °C can achieve volatilization but cannot destroy PFAS, risking the emission of fluorinated greenhouse and hazardous gasses, such as hydrogen fluoride (HF) and volatile organic fluorine (VOF) (e.g., CF₄ and C₂F₆), and products of incomplete combustion (PIC) [15] [16] [17]. PFAS toxic by-products emitted during heating are rarely monitored; this has led to the ban of PFAS incineration in some regulatory jurisdictions; this study was able to capture and analyze these by-products to provide a better understanding of the nature of those transformation products.

1.2 Research Objectives

The main objectives of this study were the following:

- 1- Evaluate the ability of heat to remediate PFAS-contaminated sand in situ over a range of temperatures (550 °C, 500 °C, 400 °C, and 300 °C) in the presence of air.
- 2- Gain knowledge about the transformation products that are released during the heating process by measuring a broad suite of targeted and untargeted PFAS
- 3- Complete fluoride mass balances to better understand PFAS fate during thermal remediation.
- 4- Check the possibility of reforming longer fluorinated chain from shorter chain PFAS radicals formed during heating.

5- Identify any new classes of PFAS transformational products using advanced analytical techniques to characterize different PFAS released during thermal remediation.

By achieving these objectives, this study will lend itself to improving existing thermal remediation technologies, which will lead to a better mitigation approach. Results from these experiments may provide a fundamental understanding which can be built upon to improve thermal remediation approaches and maximize the destruction of PFAS.

1.3 Thesis Outline

This thesis is written with the guidelines and regulations stipulated by the School of Graduate Studies at Queen's University Kingston. Chapter 2 is a general review of the available literature that gives a background about PFAS diversity, environmental behavior, contamination sources, and a review of the most common remediation technologies.

Chapter 3 presents the results from laboratory experiments exploring the ability of heat to remove PFAS from contaminated sand. This chapter is written in a thesis format that will later be adjusted to be written in a manuscript format for the intention of submission to a peer-reviewed journal.

Chapter 4 summarizes the research performed, the conclusions from this work, and recommendations for future continuing work. Appendices provide additional information mentioned throughout the thesis. Samer Al-Dirani is the author of all chapters in this thesis.

Chapter 2

Literature Review

2.1 PFAS Diversity

PFAS are fluorinated organic chemicals oil and water-repelling and contain hydrophilic and lipophilic functional groups [18]. In polyfluoroalkyl substances (polyFAS), at least one (but not all) hydrogens have been replaced by fluoride, while in perfluoroalkyl substances (perFAS), all hydrogens have been replaced by fluoride [18].

PFAS can also be classified as polymers and non-polymers. Polymeric PFAS can be categorized into three sub-groups: fluoropolymers, perfluoropolyether, and side-chain fluorinated polymers. Nonpolymeric PFAS are within four subfamilies: perfluoroalkyl acids (PFAAs), fluorotelomers (FTs), pre-and polyfluoroalkyl ethers (PFPEs), and other compounds derived from perfluoro alkane sulfonyl fluoride (PASF). The most common classes of PFAAs are perfluorosulfonic acids (PFSAs) and perfluoroalkyl carboxylic acids (PFCAs). Among PFAAs, perfluorooctanoic acid (PFOA) and perfluorooctanesulfonic acid (PFOS) are the most detected PFAS in environmental samples. Table 1 summarizes the physical and chemical properties of PFOA and PFOS.

Table 1: Physical and chemical properties of PFOA and PFOS [19]

Properties	PFOA	PFOS
Molecular weight (g.mol ⁻¹)	500.13	414
Molecular formula	C ₈ HF ₁₇ O ₃ S	C ₈ HF ₁₅ O ₂
Melting point (°C)	> 400	45–50
Vapor pressure at 20 °C (mm Hg)	2.48 x 10 ⁻⁶	0.017
Water solubility at 25 °C (mg. L ⁻¹)	550–570 (purified water)	9.5 x 10 ³
pKa	2.80	-3.70
Organic-carbon partition coefficient (log K _{oc})	2.57 (estimated based on anion and not the salt)	2.06

PFAS varies in length and may include linear or branched isomers [20]. Short-chain PFAS are PFCAs with less than seven carbons, whereas PFSAAs have less than six carbons. PFAS isomers are classified as linear if they have a carbon atom bonded to one or two other carbons with homologs of varying $-CH_2-$ groups, whereas branched isomers have their carbon backbone bonded to more than two carbon atoms with homologs of variable $-C_2F_4-$ groups. In most environmental samples, PFAS are found as a mixture of linear and branched isomers and short and long chains.

Based on their environmental media, PFAS can be neutral or ionic. The pKa values (Table 1) show that PFCA and PFSA are strong acids and exist as dissociated anions of acids under natural soil conditions. However, because of their surfactant nature, the pKa values depend on the concentration of PFAS. Burns et al. (2008) revealed that monomeric PFOA pKa is 3.8 but can be as low as -0.2 due to perfluorooctanoate (PFO) aggregation [21].

Each PFAS behaves differently depending on chain length, functional head, and other characteristics. These differences stem from two manufacturing routes, the electrochemical fluorination (ECF) and the fluorotelomer process (FT). ECF results in a mixture of linear and branched isomers with even and odd numbers of PFAS. Whereas the telomerization process creates linear isomers with an odd number of partially fluorinated compounds [22].

Table 2 lists the structure and properties of the most studied PFAS.

Table 2: The most studied PFAS in the literature [23]

Compound Name	Molecular Formula	Solubility (mg.L ⁻¹)	Vapor Pressure (Pa)
Perfluoroalkyl Carboxylic Acids (PFAAs)			
Perfluoroalkyl Carboxylic Acids (PFCAs)			
perfluorobutanoic acid (PFBA)	C ₃ F ₇ CO ₂ H	851 (25 °C)	
perfluoropentanoic acid (PFPeA)	C ₅ HF ₉ O ₂	-	-
perfluorohexanoic acid (PFHxA)	C ₆ HF ₁₁ O ₂	-	-
perfluoroheptanoic acid (PFHpA)	C ₇ HF ₁₃ O ₂	118,000 (21.6 °C)	20.89 (25 °C)

perfluorooctanoic acid (PFOA)	C ₈ HF ₁₅ O ₂	4340 (24.1 °C)	4.17 (25 °C)
perfluorononanoic acid (PFNA)	C ₉ HF ₁₇ O ₂		1.29 (25 °C)
perfluorodecanoic acid (PFDA)	C ₁₀ HF ₁₉ O ₂	260 (22.4 °C)	0.23 (25 °C)
perfluoroundecanoic acid (PFUnDA)	C ₁₁ HF ₂₁ O ₂	92.3 (22.9 °C)	0.10 (25 °C)
perfluorododecanoic acid (PFD _o A)	C ₁₂ HF ₂₃ O ₂	-	0.008 (25 °C)
Perfluoro Sulfonic Acids (PFASs)			
perfluorobutane sulfonic acid (PFBS) (C ₄)	C ₄ HF ₉ O ₃ S	510	-
perfluorohexane sulfonic acid (PFH _x S) (C ₆)	C ₆ HF ₁₃ O ₃ S	-	-
perfluorooctane sulfonic acid (PFOS) (C ₈)	C ₈ HF ₁₇ O ₃ S	570	3.31x10 ⁻⁴ (25 °C)
Precursor Compounds			
Fluorotelomer Alcohols (FTOHs)			
4:2 fluorotelomer alcohol (4:2 FTOH)	C ₄ F ₉ CH ₂ CH ₂ OH	974 (22.5 °C)	992 (25 °C)
6:2 fluorotelomer alcohol (6:2 FTOH)	CF ₃ (CF ₂) ₅ (CH ₂) ₂ OH	18.8 (22.5 °C)	713 (25 °C)
8:2 fluorotelomer alcohol (8:2 FTOH)	C ₇ F ₁₅ CF ₂ CH ₂ CH ₂ OH	0.194 (22.3 °C)	254 (25 °C)
10:2 fluorotelomer alcohol (10:2 FTOH)	C ₁₂ H ₅ F ₂₁ O	0.011	144 (25 °C)
Per fluoroalkane Sulfonamides (FASAs)			
perfluorooctane sulfonamide (FOSA)	C ₈ H ₁₈ FNO ₂ S	499.14	2.56
N-alkyl Perfluoroalkane Sulfonamidoethanols (FASEs)			
N-methyl perfluorooctanesulfonamidoethanol (N-MeFOSE)	C ₁₁ H ₁₀ F ₁₇ NO ₃ S	0.81 (25 °C)	0.70 (25 °C)
N-ethyl perfluorooctane sulfonamidoethanol (N-EtFoSE)	C ₁₂ H ₁₀ F ₁₇ NO ₃ S	0.89 (25 °C)	0.3525 °C)

2.2 Sources of PFAS in Soil

Table 3 lists previously published statistics for PFOA and PFOS distribution in surface and subsurface soil. PFOS was the predominant PFAS detected, and PFOA was also detected in both media, but concentrations were generally much lower. The concentration of PFAS in soil from each site varies and depends on the initial exposure type. For example, high exposure was detected

in AFFF testing and manufacturing areas, medium exposure in hangars and buildings, and low exposure in AFFF emergency use areas. Therefore, a high degree of variability can be observed, reflecting site-specific conditions and operational practices.

Table 3: Summary statistics for PFOA and PFOS measured by matrix [24]

Summary Statistics for PFOA and PFOS Measured by Matrix			
PFAS	Parameter	Surface Soil (ppm)	Subsurface Soil (ppm)
PFOA	DF	79.12%	48.08%
	Median ²	1.45	1.55
	Maximum	58.0	140
PFOS	DF	98.90	78.85%
	Median ²	1.20	0.470
	Maximum	620	160

² Median values are reported using only detected concentrations
Abbreviations: DF = detection frequency

2.2.1 Firefighting Foams

Historically, aqueous film-forming foams (AFFFs) contained long-chain PFAAs, but in 2015, the foam manufacturers eliminated long-chain PFAAs from their products. Current AFFF formulations contain fluor surfactants that can transform into shorter-chain PFAAs. Shorter chains are considered less toxic and less bio-accumulative [1]. However, they are highly persistent and mobile, and necessary soil cleanup is prohibitively expensive.

Hydrofluoric-based foams may be released while extinguishing fires or spillage during storage and handling. In the United States, most PFAS-impacted areas are at military facilities where AFFFs were used for firefighting purposes. A previous investigation of AFFF-impacted groundwater at firefighting training areas associated with the US military showed that PFOS and PFHxS are the dominant PFAS detected, followed by PFOA [2]. In addition, strong evidence has linked telomer-based AFFFs to PFCA presence [25].

2.2.2 Wastewater

Wastewater treatment facilities are primary sources of PFAS. Short-chain PFAS are becoming more common from these sources since the phasing out of long-chain fluor-surfactants. For example, high concentrations of short-chain PFAS were detected in the surface water of Tangxun Lake in China [26]. PFBA and PFBS were the predominant forms, with average concentrations of $4.77 \mu\text{gL}^{-1}$ and $3.66 \mu\text{gL}^{-1}$, respectively. The source of the short-chain PFAS was untreated industrial water.

PFAS was also detected at many waste disposal sites. Short-chain PFAS were detected at many rural dumping sites and municipal wastewater stations [27]. Each site was contaminated with different PFAS, indicating that each source contributed to different PFAS profiles.

Industrial wastewater treatment plants can also contribute substantial amounts of PFAS. Various data show that wastewater treatment plants discharge up to 50 times more PFAS than they receive in municipal wastes, and that PFOA in the wastewater effluent was 325% greater than that in the influent [28] [17]. The source of PFAS in the effluent are precursor compounds that degrade into PFAS. However, the concentrations of PFOS and PFOA can decrease in the effluent, which may be attributed to the high distribution constant (K_d) causing molecular retention in the sludge and decreasing PFOS concentration in the effluent [29].

2.2.3 Landfill Leachate

Various PFAS, such as PFBA, PFH_xA, and PFHpA, are currently used in consumer products, including nano sprays, outdoor textiles, carpets, gloves, paper food wrappers, and leather. Household wastes, such as those mentioned above, are usually disposed of in landfills. As a result, PFAS can be released into the groundwater through contaminated leachates from landfills or move

from the landfill areas to surrounding land if an appropriate lining is not installed. Even though landfilling is the most common method to manage PFAS-contaminated soil. However, it is becoming more unfavorable due to the restrictive regulations, high operational costs, and long-term liability.

2.3 Short-chain PFAS and Precursor Transformation

Short-chain PFAS are becoming more common as long-chain compounds have been phased out of use. Short-chain PFAS such as PFBA, PFH_xA, and PFHpA can be found in outdoor textiles, carpets, gloves, and food packaging [30]. Some short-chain PFAS can also be derived from natural transformations. For example, the atmospheric degradation of hydrofluorocarbons (HFCs) and hydrochlorofluorocarbons (HCFCs) can produce trifluoroacetic acid (TFA).

In addition to the widespread use of shorter chain PFAS in the environment, other sources of PFAS are precursor compound degradation, such as FTOHs, FASAs, N-MeFOSEs, and Fluorotelomer carboxylic acid (FUTCAs) [31]. Studies have shown that FUTCA can oxidize and transform into PFAS with a similar or shorter carbon chain length. For example, 6:2 FUTCA can transform into PFH_xA and PFPeA, and 8:2 FUTCA can degrade and form PFOA with slight traces of PFHpA and PFH_xA [31]. A recent study for 6:2 FTOH biotransformation in river sediments over 100 days detected nine different transformation products. 6:2 FTOH half-life was approximately 1.8 days, indicating that the microbes found in sediment can rapidly transform 6:2 FTOH into poly- and perfluorinated carboxylic acids. The predominant polyfluorinated acids on day 100 were 5:3 acid (F(CF₂)₅CH₂CH₂COOH), in addition to smaller quantities of PFPeA, PFH_xA, and PFBA [32].

Precursor transformation can sometimes depend on the organic content present in the soil. Kim et al. (2012) studied the biotransformation of 4:2 FTOH by *P. oleovorans* over 48 h in the presence and absence of n-octane. The results show that in the absence of n-octane, showed greater bio-

defluorination. The presence of n-octane limited biotransformation almost by twofold, acting as the main carbon source for *P. oleovorans* instead of FTOH [33].

Another form of precursor transformation is the interaction of living organic matter in the soil with PFAS. For example, the uptake and metabolism of 10:2 fluorotelomer alcohol in soil-earth worm and soil wheat showed that 10:2 FTOH could biodegrade to products such as PFOA, PFNA, and PFDA in soil. In addition, 10:2 FTOH can accumulate and transform into PFNA and PFDA in earthworms. Proving that precursor degradation could be a significant potential source of PFCAs in the environment [34].

Wastewater treatment plants can also act as a medium for precursor transformation. Effluent samples examined from a wastewater treatment plant showed that PFAA precursors were present in all samples and accounted for 63% of the total PFAS molar concentration. Most precursors that were produced are PFBA, PFPeA, PFHpA, PFHxA, and PFHxS [35].

All the previously mentioned studies demonstrate that precursor compounds could act as an ongoing source of PFAS, particularly short-chain PFAS. This addresses the critical need for a remediation technology that can destroy PFAS regardless of the by-products and precursors present. Thermal remediation has always been considered an option to eliminate emerging contaminants irrespective of the chemical species present. However, when it comes to PFAS, it is an entirely different dynamic since PFAS can transform into various compounds that are not fully understood.

2.4 Biological Effect of PFAS Exposure

PFAS are considered critical compounds in environmental toxicology studies. Both human and animal epidemiological data suggest that early exposure to PFAS can impact human health by

causing changes in lipid metabolism, leading to delays in development, specifically mammary gland development. Rodent's studies showed that exposure to PFAS during the late-gestation period could drastically increase the risk of newborn fatality and impact body and relative liver weight. Some studies have reported a link between PFOA exposure and kidney and testicular cancer [36]. For example, a case study showed that cancer cases increased with a reported increase of PFOS and PFOA in the serum [37].

Most PFAS toxicity knowledge stems from PFOS and PFOA studies, but this may not be a good representation of all PFAS; there is a need to study the toxicity of PFNA, PFHxS, PFBA, and short-chain PFAS, since they have been used as replacements for PFOA and PFOS. For instance, an animal laboratory study showed that high exposure to PFBA (up to 100 mg.kg⁻¹) at a young age could increase thyroid and liver weight, decrease red blood cell count, and reduce cholesterol levels [38].

Even though the toxicological data on long-chain PFAS is very well established, most current toxicological information has been performed on animals. More field data should be conducted on human exposure. Health risk data can provide critical scientific bases to accelerate the regulation of short-chain PFAS since they can spread faster in the environment and contaminate larger areas. However, as this study indicates, unknown and undiscovered PFAS with undocumented toxicological or biological data were by-products of PFOA and PFOS thermal degeneration.

2.5 Environmental Behavior of PFAS in Soil

PFAS compounds that reach soil can undergo sorption, partitioning, and complexation reactions, allowing them to be retained in the soil for long periods. Sorption referred to the electrostatic interaction between PFAS and charged clay matter, whereas partitioning is the hydrophobic interaction between the PFAS molecule and organic substrate (soil organic content). Complexation

refers to partitioning PFAS with dissolved organic matter to form a soluble PFAS-organic solution [39].

The behavior and fate of PFAS in soil depend on the characteristics of the PFAS compounds (including solubility and functional ionic head), the soil properties (organic content and pH), and some environmental factors (e.g., precipitation).

PFAS compounds can adsorb onto soil particles through hydrophobic interaction and electrostatic attraction [40] [41]. The long-fluorinated alkyl chains of PFAS compounds provide their hydrophobic properties, whereas the sulfonate and carboxylate functional ionic heads endow them with hydrophilic characteristics [42] [43]. Due to the low Henry's Law constant value of PFAS, the vapor state mobility of PFAS compounds is highly unlikely under typical soil conditions. However, short-range atmospheric transport and deposition can occur with shorter chain PFAS. Released PFAS can likely get tied to particulate matter, which settles to the ground during rain or dry weather. That is why it was important for this study to analyze and quantify various PFAS released by the emissions during thermal remediation.

2.5.1 Properties Affecting PFAS Sorption and Desorption Behavior

Two main mechanisms of PFAS sorption have been identified: (1) hydrophobic interactions of PFAS with soil particles rich in aromatic hydrophobic components (i.e., organic matter), and (2) electrostatic interactions with charged materials on the soil surface [44].

The main property affecting the strength of PFAS sorption is the organic content of the soil (f_{oc}). Higher organic content leads to a greater PFAS sorption [13]. When the sorption behaviors of PFOA and PFOS were evaluated on five different soils with variable fractions of organic carbon. The results showed that the absorbed concentration of both PFOA and PFOS increased with increasing soil organic content. In addition, K_d values between the soil and aqueous PFOA and

PFOS solution were calculated over various concentrations. Results showed that the K_d value of PFOS was greater than that of PFOA for all soil types, and the soil with the highest f_{oc} had the highest affinity for PFOA and PFOS. For multiple soil types, a linear relationship exists between f_{oc} and K_d of PFOA and PFOS [45]. In addition, increasing the organic matter in the aqueous PFOA and PFOS solution negatively affects PFAS sorption onto the soil. For example, PFOA and PFOS K_d values decreased with increased humic acid concentration. This can be related to the formation of complexes between the PFAS and organic functional group of the humic acids in the soil solution, which can inhibit the sorption of PFASs to the organic matter present in the soil [45].

Experiments also found that the sorption of PFAS to soil tends to increase with higher ionic strength and low pH of the soil [46]. Higher electrolyte concentration (e.g., calcium ion Ca^{2+}) and higher valent cations in the soil solution were correlated with an increase in the sorption capacity of PFAS onto the soil. The low pH of the soil increases the dominance of positively charged protons (H^+) on the soil surface, allowing for stronger electrostatic interactions with the positive charge on the soil particle and the functional ionic head of the PFAS [43] [47]. Tang et al. (2010) found that the adsorption of PFOS onto goethite strongly relates to pH and ionic strength. For example, at a background electrolyte concentration of 1 mM, adsorption increased from 0 at pH 9 to $6.2 \mu g \cdot m^{-2}$ at pH 3. However, high adsorption of PFOS was achieved on silica sand regardless of the solution pH and ionic strength, even though charged silica surface is negative and should result in electrostatic repulsion. The authors hypothesized that the adsorption of PFOS molecules might be primarily driven by the hydrophobic interactions between PFOS tails and hydrophobic moieties on the silica surface [48].

Sorption is also affected by the carbon chain length and sulfate moiety. Longer chain PFAS adsorb in soils and sediment mainly through hydrophobic attraction. Each additional CF_2 moiety will increase sorption, where the interaction is stronger in PFSA than in their PFCA analogs [13].

Shorter chain PFAS tend to adsorb via polar-polar interactions [49]. Laboratory experiments simulated the effect of precipitation on the migration of PFAS from soil to groundwater using flow-through 60 cm columns. Shorter chained PFAS (less than seven carbons) were more mobile than longer chain PFAS molecules. The leaching behavior was also related to the organic content of the soil. When the organic content was approximately 2%, PFOS was detected in leached water after 70 weeks, whereas PFBA and PFBS were seen after only seven weeks. By increasing the organic content of the soil to 14%, the PFOS required more than two years to be eluted [50] [51].

In addition, site characterization parameters, such as inorganic content, dissolved organic carbon, and co-contaminant distribution, can also affect the occurrence and distribution of PFAS. Studies have found that perfluoroalkyl acid (PFAAs) sorption mechanism in the soil at previous AFFF-impacted firefighting sites was influenced by other nonfluorinated surfactants, fuels, and chlorinated solvents [52]. It was shown that non-aqueous phase liquids could act as an additional sorbent to PFAAs and block the sorption of PFAA into other organic matter in soil with low organic content.

Therefore, we can conclude that the remediation of PFAS contaminated soil is extremely challenging. Thermal treatment techniques have been tested at the field scale. However, many of those field-scale studies focus on post-treated soil without taking into consideration the emissions being released. That is why this study focuses on characterizing PFAS emission to provide better emission control and understand the type of contaminants that are being released.

2.6 PFAS Remediation Strategies

PFAS treatment technologies can be divided into two categories: (1) destructive and (2) non-destructive. Destructive technologies cause PFAS to chemically transform, ideally causing a reduction in their toxicological characteristics. Most destructive technologies use heat or oxidizing

agents. The two categories of non-destructive technologies are removal and immobilization. Removal can occur via soil excavation, soil flushing, or pumping of the PFAS leachate for later treatment. Immobilization leaves the PFAS in the soil but prevents further spread into the underlying subsurface by contaminant bonding with the soil matrix.

PFAS-contaminated water has been the subject of many more studies than PFAS-contaminated soil [9]. What applies as an effective treatment for water cannot be assumed appropriate for contaminated soil. In situ technologies such as air sparging, soil vapor extraction, and biodegradation have been proven ineffective as PFOA and PFOS have low Henry's Law constants [53] [42]. Due to their carbon fluoride bond, the stability of PFOA and PFOS also causes chemical oxidation and biological methods to be ineffective as treatment technologies. The following section lists the most common and effective PFAS treatment technologies in soils.

2.7 Non-destructive Remediation of PFAS-contaminated media

2.7.1 Immobilization/Sorption

Immobilization uses liquid chemical solutions or absorbing agents such as those used in water treatment to prevent the leaching of PFAS from the soil. Some of the most common materials for adsorbing PFAS in soil include carbon-based and clay-based substances, ionic surfactants, and anion exchange resins.

The nonpolar functional group makes it useful for hydrophobic PFAS sorption for carbon-based material. Carbon-based materials can be further classified into three groups: (1) granular activated carbon (GAC), (2) powdered activated carbon (PAC), and (3) multiwalled carbon nanotubes (CNTs). CNTs have the highest sorption capacity of these carbon-based materials, followed by PAC. For example, CNTs demonstrated a faster PFOS adsorption equilibrium (2 h) than other sorbing materials such as biomass-derived chars (384 h) and ash (48 h). This is due to the higher

number of available reaction sites on the external surface of the CNTs and strong hydrophobic interactions [54].

Mineral options for PFAS sorption include organoclays (organically modified clay, montmorillonite, kalinite, and palygorskite), iron oxide (goethite, hematite), and silica. In most cases, natural clay minerals have a hydrophilic surface that is negatively charged, making them ineffective for anionic and hydrophobic PFAS removal. However, modifications with surfactants and ammonium or amino groups can enhance their sorption capacity. Laboratory studies have shown that quaternary ammonium surfactant-modified products could generate a positive charge surface, possibly trapping PFOA and PFOS via electrostatic interactions [55]. Das et al. (2013) reported a modified clay absorbent that can immobilize PFOS in contaminated soil. The absorbent was made of a palygorskite-based organoclay modified with oleylamine, commercially known as MatCARE™. The effectiveness of this absorbent in immobilizing PFOS was examined. First, the initial PFOS concentrations of four different soils from sites impacted by AFFF were measured, and 10 grams of MatCARE was applied to 100 grams of sand. Without MatCARE, the average amount of PFOS released after one year at 25 °C was 8.14%. In comparison, with the application of MatCARE, no detectable PFOS was released. The experiments were also conducted on PFOS lab-spiked soils, and the average concentration of PFOS release decreased from 18% in the untreated sand to almost 0.15% for the treated sand [56].

Liquid-based absorbents have recently been studied to immobilize PFAS in contaminated sand. Various methods have been tested for increasing PFAS sorption to aquifer solids by adding commercially available drinking water coagulants. The coagulants can increase the PFAS sorption capacity from the soil by a factor of 2.0–6.1. However, PFAS sorption using this method is not readily reversible [57].

Many factors such as the soil organic content, adsorbent properties, and co-contaminant presence will influence the effectiveness of Immobilization as a treatment technology. For example, the adsorption of PFCs on activated carbon decreases significantly during the treatment of contaminated water. However, adsorption was improved considerably when the water was directly pretreated with H₂O₂ oxidation to remove most organic matter except PFAS, indicating that organic matter is a competitive source for PFAS adsorption [58]. In addition, adsorbent properties, such as particle size, pore size, and surface chemistry, also remarkably affect PFAS sorption. Adsorbents with smaller-sized particles have superior adsorption. Similarly, adsorbents with mesopores and macropores are better for diffusion and adsorption of PFOA and PFOS. Adsorbents with more basic groups can adsorb more PFCs through hydrophobic and electrostatic interactions [59].

Battista et al. (2020) assessed the diffusive behavior of PFOA and PFOS through linear low-density polyethylene (LLDPE) and LLDPE coextruded with ethyl vinyl alcohol (EVOH). The study was performed for concentrations below and above 0.001 critical micelle concentration at temperatures of 23°C, 35°C, and 50 °C. The study showed that minimal diffusion through both membranes occurred, with the coextruded membrane exhibiting low diffusivity of PFOA and PFOS. In addition, this study proved that hemi-micelle and micelle formation of PFOA and PFOS does not affect the diffusion properties of the membrane [60].

The previously mentioned studies show that the immobilization of PFAS can be a complex process, with efficacy varying with soil properties and molecular properties of the individual PFAS. Unlike thermal remediation, immobilization strategies must be adjusted to site-specific conditions and contamination profiles.

2.7.2 Phytoremediation

Phytoremediation of organic pollutants usually consists of three main mechanisms: (1) phytofiltration (plant uptake), (2) phytovolatilization (conversion of pollutants to volatile form), and (3) phytodegradation (participation of root exudates and microbial population). However, since PFAS are resistant to photolysis and have limited biodegradation, plant uptake may be the primary route for site remediation. PFAS from the soil is mainly transported into the plant roots via passive (diffusion) and active processes [61]. Passive transport is the diffusion of small, non-ionized PFAS driven by the plant's transpiration stream. When PFAS enter the roots, they will be translocated to the stems, shoots, leaves, and fruits. However, active transport is a selective adsorption process in which PFAS are picked up by carrier proteins, aquaporin channels, and anion channels to be transported into the plant cell [62]. One important metric in assessing bioaccumulation and translocation of PFAS in plants is the bioconcentration factor (BCF) [63]. BCF indicates the affinity of PFAS for bioaccumulation in different plant organs. Hyperaccumulation of PFAS compounds in plants occurs when the BCF value is greater than 10.

One major factor for plant bioaccumulation and translocation of a PFAS is its chain length. Longer carbon chain will cause an increase in the octanol-water partition coefficient ($\log K_{ow}$) and decrease the BCF. For example, pot experiments were performed to evaluate the accumulated concentration of several PFAAs within wheat cultivated in soil. The results showed higher BCF (greater than 10) for PFBA in wheat compared to PFOA which was less than 1 [64]. Another influencing factor is the PFAS functional group. PFAS with sulfonate groups exhibit stronger adsorption to the soil and less plant uptake. For example, the BCF of PFOA hyperaccumulating species ranged from 11.5 to 46.6 and that of PFOS ranged from 10.3 to 17.9 [65].

Laura et al. (2017) studied the uptake of 26 PFAS in plants from areas with elevated levels of PFAS contamination (16 ng. g⁻¹ to 160 ng. g⁻¹). Samples from the surrounding area were collected from

several plant species and tissues (i.e., roots, twigs, leaves, and trunks). The plants showed high variability of PFAS concentration with up to 97 ng. g⁻¹ and 94 ng. g⁻¹ in birch leaves and spruce needles, respectively. In addition, ground cover plants such as long beech fern, ground elder, and bird cherry bushes showed concentrations of 6.9 ng. g⁻¹, 23 ng.g⁻¹, and 21 ng.g⁻¹ w/w, respectively. The authors concluded that a shelterwood system with a mixed stand of silver birch and spruce combined with leaf harvest, birch sap, and the understory of a ground elder could remove up to 1.4 g of PFAS per year per hectare [66].

Even though bioremediation has the potential to treat PFAS. However, plants used for phytoremediation must be able to tolerate the type and the high concentration of PFAS present at any given site [67]. That is why bioremediation might take several years to clean up a site. Thermal remediation can destroy PFAS quickly regardless of the concentration and type of PFAS present.

2.7.3 Excavation and Specialized Landfills and Encapsulation

Contaminated soil can be excavated and transported to areas specifically designed for long-term containment. These areas are usually surrounded by low permeability barriers built with materials such as clay or synthetic textiles to reduce the risk of contaminant migration [68]. Treatment walls can also be installed at the original area of the contamination to act as a long-term storage area. The treatment walls are constructed by digging a trench around the contaminated plume and filling it with a material that can treat the contaminated groundwater as it passes through the barrier. The three most common treatment walls are sorption barriers, degradation barriers, and precipitation barriers.

Since PFAS are considered nonreactive chemicals i.e., they do not degrade as they pass through the treatment walls. Filling those wall barriers with a sorbent material such as activated carbon can capture the PFAS and hold them in place.

Due to the continuously evolving regulations that affect PFAS clean-up levels, fewer landfills are accepting PFAS. This strikes the need for a destructive remediation technology. Thermal remediation is considered a great technology for destroying PFAS, mainly if the emissions are adequately characterized and understood.

2.7.4 Groundwater Pump and Treat

Groundwater pumps and treat have been proven effective in treating contaminated soil leachate to prevent PFAS from being released into the drinking water supply [69]. The technology is usually accompanied by some sort of filtration or adsorption process for the pumped water.

Filtration removes PFAS from contaminated water by forcing water into a semipermeable membrane. Results have shown that reverse osmosis and nanofiltration effectively remove PFAS regardless of chain length, while ultrafiltration and microfiltration perform poorly.

GAC sorption, a hydrophobic process, is commonly used in PFAS-contaminated water treatment technologies. GAC sorption can remove longer chain PFAS but becomes less effective with shorter chain PFAS and precursors. Paterson et al. (2008) conducted a field to assess the ability of GAC to treat PFAS-impacted soil at a previous firefighting training site. The study involved the installation of an in situ multiphase vacuum extraction system. Four rotary claw pumps removed both groundwater and vapor from the subsurface. The extracted groundwater was passed into an oil-water separator and an air stripping unit and then sent into large drums to be treated via GAC.

Even though the GAC has a PFAS extraction efficiency greater than 99%, it was estimated that only 0.1% of the total PFAS in the soil was removed [70].

Such technologies have high implementation and operational costs, causing them to be cost-ineffective. The membranes used can be compromised by suspended solids and the complex geochemistry of water, which can create additional costs due to fouling. Other limitations, such as low efficiency, contamination rejection, and low flow rates, can make this technology site-specific. Most of the wastes generated (e.g., PFAS-contaminated GAC) will require additional thermal treatment at high temperatures (>1000°C).

2.7.5 Soil Flushing

Soil flushing is an in-situ process that involves the injection of a specific solution into the ground to enhance the extraction of contaminants from their binding media. Soil flushing successfully treated many contaminants, such as persistent organic pollutants and heavy metals. The advantage of soil flushing is its ability to treat large quantities of soil in situ without excavating or transporting the soil [71].

In most soil flushing cases, surfactants are the primary active extraction ingredients. Surfactants contain both a hydrophobic and hydrophilic portion. However, many PFAS, including PFOA and PFOS, are surfactants by their chemical nature, making their behavior unpredictable when coupled with a soil flushing agent. Other common flushing agents include organic/inorganic acids, bases, methanol, ethanol, and oxidizing agents.

Many studies have been performed to examine the effect of cationic and anionic surfactants on the sorption of PFOS in soil sediments. Pan et al. (2009) tested the sorption and desorption effect of the cationic surfactant cetyltrimethylammonium bromide (CTAB) and the anionic surfactant sodium dodecylbenzene sulfonate (SDBS) on PFAS sediments. CTAB was able to immobilize

PFOS effectively regardless of the surfactant concentration. They suggested that CTAB may have adsorbed to the sediment first, thus exposing its hydrophobic tail and acting as a PFOS sink. However, the anionic surfactant SDBS had a concentration-related effect. When the SDBS concentration was lower than 4.3 mg. L⁻¹, PFOS sorption to the soil increased. For concentrations between 21 mg. L⁻¹ and 44 mg. L⁻¹, PFOS sorption decreased. Therefore, the authors concluded that SDBS at high concentrations could be used as an effective surfactant in improving the mobilization of PFOS in sediments [72].

Pressurized liquid extraction (PLE) is a multi-step procedure to extract fluorinated an-ionic and non-ionic surfactants in sewage sludge. PLE combined with certain solvents can be a great remediation option for PFAS. For example, solvents such as ethyl acetate-dimethylformamide and methanol-phosphoric acid (EtOAc-DMF-MeOH-H₃PO₄) showed excellent PFAS recoveries. This method was proven stable and reproducible with an extraction percentage of 100% (150 µg.g⁻¹ of sewage sludge) [73].

Soil flushing only transports the contaminant from the soil to the water (leachate). Second-stage treatment streams should be included to treat the aqueous stream and allow the water to be used again for more soil flushing. Common second-stage treatment includes liquid-liquid extraction and membrane separation [68].

2.7.6 Soil Washing

Soil washing and soil flushing employ the same physiochemical principle, in which both methods use an extraction agent in an aqueous solution to remove contaminants such as PFAS. However, unlike soil flushing, which is in situ, soil washing requires the excavation of the contaminated soils and treatment in an ex-situ unit. The first step of soil washing is the removal of the coarse component of the sand (gravel and rocks) to isolate the smaller, more refined components (clay

and silt) [68]. The rough piece of the sand usually carries little PFAS contamination; therefore, it does not require further treatment. However, fine particles are more contaminated since hydrophobic organic contaminants bind to smaller, organic-rich particles. This separation process reduces the volume of PFAS-contaminated soil that requires decontamination.

However, this remediation option must be coupled with other technologies such as incineration, bioremediation, or ball milling. Overall, soil washing is expensive, creates additional waste streams, and impractical for the large volume of PFAS-contaminated sands.

2.8 Destructive Methods for PFAS Removal from Soil

2.8.1 Bioremediation

Biodegradation uses microorganisms to remediate soils and groundwater contaminated with organic pollutants. Numerous studies have examined the biodegradation of PFAS precursors through their microbial transformation in aerobic environments. However, little research has been performed on the biodegradation of PFOA and PFOS. The biodegradability of PFAS depends on the types of microbes or microcosms present in the soil. For example, *E. coli* could not biodegrade PFOA and PFOS [74]. Whereas enrichment cultures of *Acidimicrobium* sp. strain A6 achieved removal rates up to 60% of PFOA and PFOS [75]. *Pseudomonas plecoglossicida* 2.4-D also showed a unique ability to use PFOS as the primary carbon source. When introduced to the soil, the strain biodegraded PFOS by 75%, accompanied by the release of free fluorine atoms [76]. In addition, *P. aeruginosa* could decompose PFOS over a 12-hour incubation period [77].

Most studies claim that the mechanism behind PFAS biodegradation is limited to non-fluorinated moieties. However, the aerobic biotransformation of perfluorooctaneamido quaternary ammonium salts (PFOAAs) resulted in an increased concentration of PFOA. Without microorganisms, the

PFOA concentration remained unchanged. This shows that biodegradation was possible even with the breakdown of the non-fluorinated moiety [78].

Even though some authors have reported the release of total fluoride ions of the PFOS concentration in aerobic microbial treatment, they speculate that the fluoride ion released in PFOA and PFOS bioremediation is derived from impurities present in PFOS and PFOA reagents. Without a complete fluoride mass balance, the effectiveness of such technologies remains unclear.

2.8.2 In-situ Chemical Oxidation

Conventional water oxidation methods such as chlorination, ozonation, and chemical oxidation are ineffective in treating PFAS-contaminated sites. However, few laboratory studies have demonstrated the removal of PFAS from soil and water mixtures via chemical and thermal oxidation reactions. For example, Li et al. (2012) investigated the electrochemical decomposition of PFOA in an aqueous solution over anodic mixed metal oxides Ti/SnO₂-Sb, Ti/SnO₂-Sb/PbO₂, and Ti/SnO₂-Sb/MnO₂ for 90 minutes. The results showed a PFOA (100 mL of 100 mg.L⁻¹) degradation ratio of 98.8% and a defluorination ratio of 73.9% over the Tin/SnO₂-Sb anode [79].

Some in situ chemical oxidation methods use peroxydisulfate (S₂O₈²⁻) to treat contaminated soil. Peroxydisulfate is delivered into the soil subsurface in an inactive form. A delivery system consists of a network of high-pressure injection wells and a backhoe for soil mixing [80]. Once in contact with the contaminated zone, it can be activated through ultraviolet exposure, alkaline conditions (high pH), heat, or hydrogen peroxide [81]. One study evaluated the effectiveness of persulfate oxidation in degrading PFOA using hot water at 80 °C as an activating agent. The results showed that PFOA was degraded below the detection limit after 6 hours of treatment [82]. The presence of

fluoride ions and shorter chain PFCAs in the soil post-treatment strongly indicates chemical degradation and PFSA and PFCA formation from more complex precursors.

Researchers have attempted to develop a mixture of common oxidants that can destroy PFOS and PFOA under less extreme conditions. One method uses a combination of redox and activators called a Smart Combination In Situ Oxidation/Reduction (SCISOR). This method was reported to reduce the amount of PFAS in soil by 60% after one contact phase. This redox method has been demonstrated to degrade PFOS and PFOA in multiple treatability studies using AFFF-impacted soil. However, due to the lack of characterization and the absence of high-resolution mass spectroscopy (HRMS) of the by-products released, this method was slowly discontinued.

2.8.3 Degradation of PFAS via Controlled Irradiation

Degradation of PFAS was also found to be possible via gamma irradiation [83]. PFOA, PFOS, 6:2 FTS, and thirteen different PFAS were irradiated to investigate their degradation behavior. More than 80 fluorinated transformation products were identified. Aqueous electron was the vital reactive species responsible for initial degradation. PFOS degradation led to C₄-C₉ PFCAs, indicating that longer-chain PFAS can be formed from shorter counterparts. Traces of C₃ and C₂ PFAS were also detected, but it was too low to quantify. This proves that the chain-shortening pathway is a significant transformation mechanism for PFOA and a minor transformation mechanism for PFOS. The result from this study highlights the complexity of PFAS degradation and further emphasizes the need to characterize the by-products being formed.

2.8.4 Ball Milling

In the last two decades, mechanochemical destruction (MCD), or high-energy ball milling, has been studied as an alternative to non-combustion technology for persistent organic pollutants (POP). The significant advantage of MCD is that it is generally environmentally friendly. The

milling takes place in the solid phase at modest temperatures and pressures. Even though heat is generated under ball milling conditions, heat is not the sole reaction initiation mechanism since some mechanochemical reactions occur at very low temperatures. The MCD mechanism tends to be complex. In general, two types of bond rupture processes happen under mechanical stress. The first is the disordering and amorphization of the crystal structure and conformational transformation caused by the rupture of some intermolecular bonds. The second type of MCD reaction is the deformation of valence bonds and angles under mechanical stress. Usually, bond breaking, bond reformation, and (depending on the reagent used) oxidation, hydrolysis, and other chemical reactions can occur [84].

Zhang et al. (2013) studied the mechanochemical method using a planetary ball mill to treat PFOS and PFOA in the absence of soil. Potassium hydroxide (KOH) was the best co-milling reagent, achieving nearly complete destruction of PFOA and PFOS. The final products obtained after PFOS treatment were KF and K_2SO_4 . The mass ratio between PFOS and KOH affected the fluoride recovery but did not affect PFOS destruction.

Another study degraded a range of PFAS compounds co-milled with stoichiometric amounts of La_2O_3 and thus were fully converted into LaOF, a luminescent material with various industrial applications; this method is considered a waste-to-materials method. The reaction mechanism proposed was that the ball milling process activated La_2O_3 , which promoted the oxidation of CO_2 and PFC carbonization and fluoride incorporation into La_2O_3 's lattice to form LaOF. Even though it is highly effective, La_2O_3 cannot be implemented in soil remediation due to its high cost, and the low concentration of PFAS present in the soil does not produce a significant amount of LaOF [85].

Turner et al. (2020) demonstrated that PFAS concentrations in the sand, whether artificially spiked or collected from firefighting training areas, can be reduced by ball milling. The study showed that

ball milling without any reagents is enough to reduce PFOS and PFOA concentrations by 98% and 99% in unsaturated sand, respectively. However, a co-milling reagent such as KOH is needed in water-saturated sand to improve destruction and increase reaction kinetics. When KOH was used as a co-milling reagent, 89% of fluoride was recovered from PFOS-amended sand. The theory explaining this observation is that reactive particles formed from the fracture of sand grains can react with PFAS molecules to initiate destruction and promote defluorination [86]. Ball milling is becoming more appealing as a non-thermal technology that only requires mechanical energy as an input. Ball milling was successful in treating PFA-impacted soil and hazardous waste. Further research is needed to identify how it degrades PFAS, its kinetic reaction progression, and fluoride fate.

A scale-up of the ball milling technology was performed by Battye et al. (2022). Horizontal Ball mills were used to degrade PFOS, PFOA, and AFFF spiked nepheline sand, as well as two different soil types (sand dominant and clay dominant), collected from a fire training area. High-resolution accurate mass spectroscopy identified 19 non-targeted fluorotelomer substances, including 6:2 fluorotelomer thioether amido sulfonate (FtAoS). This strongly indicates the importance of high-resolution mass spectroscopy analysis when evaluating any PFAS destruction technology [87].

2.8.5 Vitrification

Vitrification, commonly referred to as the molten glass process, uses a high-energy source to melt soil, causing pyrolysis and immobilization of all contaminants [68]. The temperatures needed for vitrification are approximately 1600 °C to 2000 °C. The advantage of operating at such high temperatures is the lack of by-products because all organic contaminants are destroyed. Electrical, thermal, and plasma methods are available to reach vitrification temperatures. Electrical is an in-situ process involving graphite electrodes inserted into the ground and passing energy into the soil.

The thermal process is ex-situ and performed in a rotary kiln. Plasma is only required when temperatures above 5000 °C are needed. Electrical and thermal methods save energy, and they can be used to target PFAS at site-specific locations without the need to reach extreme plasma temperatures.

Incineration, which is very similar to verification, is also one of the most popular PFAS thermal remediation techniques for solid waste. However, tighter restrictions are being imposed by the EPA regarding PFAS treatment via incineration since the fate and transport of PFAS during this process are not fully understood. Most incineration studies are performed under highly controlled laboratory conditions while reporting a specific number or subset of analytes. Even under these controlled conditions, several studies have reported that incineration does not release the most common PFAS, such as PFOA [88].

2.8.6 Pyrolysis and Gasification

Pyrolysis and gasification are thermal decomposition processes that convert solid hydrocarbons into combustible gas. During pyrolysis, carbonaceous materials are exposed to high temperatures (200 °C–1100 °C) without an oxidant. The materials generated from pyrolysis are usually carbon-rich and referred to as biochar.

Gasification introduces the carbonaceous materials to high temperatures (800 °C–1650 °C) in the presence of an oxidant (air) to oxidize and reform the volatile organic fraction while converting the solid mass to ash particles. Thermal treatment under a reductive environment has recently become very popular since no oxidation by-products are released [89]. Thermal destruction of PFAS under reductive conditions occurs via hydro-defluorination. The simplest transformation is converting a carbon-fluorine bond into a carbon-hydrogen bond with the assistance of various reagents and catalysts. C-F bonds tend to be strong with a bond dissociation energy (BDE) of 500 kJ.mol⁻¹, and

a thermodynamic compensation for the C-F cleavage is required. Therefore, the balance comes from forming a thermodynamically favorable element-fluorine bond; potential features include hydrogen, silicon, boron, aluminum, or transition metals [11]. Sometimes H₂ is used as a hydrogen source since it is inexpensive, readily available, and can be derived from clean sources. When H₂ is directly introduced into the thermal reactor, the process is called gas-phase reduction, which is used extensively to treat other contaminants, such as polychlorinated biphenyls and surface contaminants [90]. One problem with treating PFAS at high temperatures is the inability to maintain PFAS within the hot zone or contaminated media before it volatilizes and exits.

2.8.7 Smoldering Combustion

Smoldering is a new thermal PFAS remediation technique. A flameless oxidation reaction is achieved by mixing fuel with inert media like sand or GAC in the presence of upward airflow (oxidant). Hydrocarbon-contaminated soil can sometimes be used as the fuel for this process, making it very energy and cost-efficient [91]. Sometimes when the organic hydrocarbon content in the soil is low or too volatile, the soil can be spiked with a surrogate fuel such as vegetable oil or wood chips. Smoldering has been used to treat wastewater solids with solid content as low as 20% by optimizing the forced airflow to account for process and feed characteristic fluctuations [92]. Smoldering can reach temperatures up to 1200 °C depending on the fuel type and concentration and the location in the reactor column. Few studies have examined the use of smoldering to treat PFAS-contaminated soils. However, most of these studies used a surrogate fuel since PFAS concentrations in soil are too small to act as a fuel [93].

In most thermal studies, emissions were not adequately analyzed. However, Duchesne et al. (2020) were one of the few studies that quantified the fate of PFAS and fluorine in sand and emission analysis to close the fluoride mass balance.

2.8.8 Hydrothermal Liquefaction

Hydrothermal liquefaction (HTL) subjects solids to moderate temperatures (280 °C–370 °C) and high pressures (10 and 25 MPa) to produce bio-oil or bio-crude. Sometimes, the process is fed dewatered slurry solids to produce bio-crude with a high heating value [94]. Many PFAS molecules produced from HTL are unstable and highly reactive and can recombine with smaller molecules to form larger ones. Yu et al. (2020) applied HTL to five targeted PFAS in aqueous-only and wet sludge samples. More than 98% of the PFOA and 8:2 FTUCA were degraded, with defluorination increasing from 19% to 30% when the reaction temperature increased from 260 °C to 300 °C. However, after the HTL was completed, the PFAS compounds and the defluorinated product were distributed in the oil and not the aqueous fraction, requiring further purification of the crude oil since they represent a primary sink for undegraded PFAS residuals [95].

2.9 Thermal Destructive Technologies

2.9.1 In Situ Thermal Treatment Technologies (ISTT)

In situ Thermal Treatment (ISTT) typically includes thermal conductive heating (TCH), electrical resistance heating (ERH), and steam-enhanced extraction (SEE). TCH involves heating the subsurface through thermal conduction via heating wells. In ERH, the heating is produced by passing an electric current through the subsurface. SEE relies on steam flow through the porous media and is highly dependent on permeability variation in the subsurface. For example, in a layer of low permeability, steam cannot penetrate low-permeability soils. In contrast, TCH and ERH technologies can be applied to contaminated media with a lesser influence on soil heterogeneity [96].

2.9.2 In Situ Thermal Technologies for Destroying PFAS

PFAS-contaminated soil was obtained from a former firefighting training area to evaluate the extent of PFAS reduction over a range of temperatures [17]. PFAS was separated into four test groups and heated using a temperature-controlled oven at 220 °C and 400 °C for 14 days and 300 °C and 350 °C for 10 days. Analysis of untreated soil revealed that the baseline concentration of PFOS was 21 ppm.

No PFAS volatilization was observed at 220 °C when the sample was heated for 14 days. At 400 °C for 14 days, the PFAS was reduced in soil by 99.998%. Short-chain PFAS such as PFBA, PFPeA, PFBS, PFHxA, and PFHpS were detected in the post-treatment sand at concentrations lower than 0.07 ppb. Heating the soil samples to 350 °C for ten days resulted in a 99.91% PFAS reduction. These results demonstrated that 350 °C might be a viable target temperature for PFAS thermal treatment and result in significant cost savings compared to temperatures above 350 °C. A lower PFAS reduction was observed at 300 °C than at 350 °C. Crownover et al. (2019) also showed that the sulfonate-based PFAS did not volatilize as readily as carboxylate-based PFAS. This observation is consistent with data indicating that the boiling points of PFCAs are generally lower than those of PFSA [17].

Söregård et al. (2020) evaluated the thermal desorption of PFAS on two different fortified soils (loamy and clay-sand), and one field of contaminated soil (clay sand) collected from a former firefighting station. The results indicated that the PFAS fraction removed from the soil generally increased with increasing temperature but depended on the soil type, initial concentration, and PFAS properties. Heating the fortified clay and loamy sand at 350 °C resulted in > 99% removal of PFCAs and FOSAs, but only 51% and 66% of (the PFSA) PFHxS and PFOS, respectively. At 450 °C, more than 99% removal for all PFAS was observed in loamy sand and clay sand-fortified soil. As mentioned in section 0, this evidence demonstrates that the PFAS functional group is an essential factor governing its desorption behavior.

In contrast to the fortified soil, the amount of PFAS removed from the field-contaminated clay sand was lower for all treatment temperatures [97]. At 350 °C, the removal of 9 different PFAS was 43% compared to 87% and 71% for the fortified sand and clay soil, respectively. At 450 °C, 99% of all PFASs (PFHxS, PFOS) were removed from the field-contaminated soil and fortified soil. At 550 °C, greater than 97% of PFPeA was released, but only 71%–93% of PFCAs were removed from the field-contaminated soil. The lower desorbing potential of PFAS in the field-contaminated soil than in the fortified soil could be related to the lower PFAS concentration or the stronger PFAS sorption in the field soil. Some shorter chain PFCAs showed negative removal at 150 °C–450 °C in the field-contaminated sand. The authors proposed that the precursor compounds could degrade and transform into PFBA. They suggested that the optimum PFAS treatment time and temperature that reduces energy demand is between 350 °C and 450 °C.

Most thermal remediation laboratory setups discussed earlier do not address the potential PFAS by-products that can form in the emission during the heating of PFAS. Incineration of PFAS can release a plethora of unidentified and unreported materials. More studies are needed on the PFAS breakdown species that could form because of products of incomplete combustion (PIC).

Chapter 3

Laboratory and Modelling Study Evaluating Thermal Remediation of PFOA- and PFOS-impacted Sand

3.1 Background

For the thermal mineralization of PFAS in contaminated sand, enough thermal energy should be introduced to drive PFAS into their thermodynamic endpoints of CO₂, H₂O, HF, or sulfur compounds. However, the chemical composition of sand is not homogenous, and compounds such as salts, minerals, and halogens can interfere to form other fluorinated, organic, and inorganic compounds. Additionally, heat zone failure is possible, the most common of which is thermal quenching by pockets of cold areas caused by flowing water if the surface analysis is inadequate. Theoretical investigation of the thermal destruction of one or two highly fluorinated carbon organic under combustion shows that C-F has a high bond strength (Table 4) [16].

Table 4: Relevant bond energies for some fluorinated compounds

Bond	Energy (kJ.mol⁻¹)
CF₃-F	552
CF₂-F	352
CF-F	508
H-F	569
F-F	159
HO-F	216
O-F	220
CF₃-H	456
CF₃-CF₃	408

Fluorinated compounds can be decomposed with a 1,2 or 1,1 elimination of hydrogen fluoride. Studies have shown that as larger fluorinated hydrocarbons degrade into smaller ones, those compounds demonstrate increased stability, requiring higher temperatures to break down. For example, CF₄ is considered very stable, such that its destruction guarantees the destruction of 99.99% of other fluorinated organic compounds. Therefore, tracking CF₄ might help determine the destruction efficiency of fluorinated compounds. However, this study shows that in the case of PFAS, tracking CF₄ is insufficient due to the complex nature of PFAS [16].

Several thermal treatment technologies are being implemented for wastewater solids contaminated with PFAS. The increased adoption of thermal treatment as a remediation method originated from improving wastewater, solid management, and energy efficiency.

PFAS thermal remediation studies have shown that PFAS highly depends on applied temperature, soil type, initial concentration, and PFAS properties [17] [97]. However, this research only focused on the effect of temperature and initial concentration on PFOA and PFOS destruction. The following study also attempts to close fluorine mass balance and analyze emissions released to better control sites where thermal remediation is in place.

3.2 Delimitations

The following experiments assessed the thermal remediation method for PFAS-laboratory contaminated sand. PFOA and PFOS were evaluated during the experiments even though these represent a small fraction of the large PFAS group, which consists of almost 3000 substances.

3.3 Material and Methods

3.3.1 PFAS Spiked Sand Preparation

Stock solutions were prepared for each experiment by mixing PFOA (98%, CAS# 335-67-1) and PFOS (97%, CAS 1763-23-1) purchased from SynQuest laboratories with 1000 mL of deionized water in one-liter polypropylene bottles. The stock solution was then placed on a shaker for 48 hours at 170 revolutions per minute (rpm). The content of each stock solution was then added to 3 kg of silica sand (AGSCO Corporation, 40/70, density = 2.65 g/cm) and placed on a shaker to completely dry. Individual batches of contaminated sand were created for each experiment. For mass balance and analytical purposes, only ~25 mg of PFOA and ~25 mg of PFOS were initially present in the sand for all temperatures regardless of the initial concentrations. Triplicate pre-treatment and post-treatment contaminated sand samples were collected, analyzed, and averaged for each experiment.

3.3.2 Heating Cylinder Apparatus

One custom-made one-liter cylinder was fabricated to hold sand during the heating experiment. The cylinder was made of a single 10.2 cm inner diameter and 13.2 cm long stainless-steel tube with two removable endplates (Figure A.1). The cylinder had four connections in the top plates, two used to connect thermocouples (TC) (Omega TJ36-CASS-14U-6-CC-XCIB), one to connect to an external air line supplying air to the cylinder using a mass flow controller (FMA-1608A, Omega Ltd.), and one to connect to a 0.25-inch outer diameter copper outlet tube to capture emissions.

The cylinder was heated in a convection oven (Carbolite Gero). The copper tube transporting the released emissions was threaded through an opening on the side of the oven. The emissions temperature leaving the oven was monitored using T-type TC (Omega, SA1XL-T). The copper

tube carrying the emission from the cylinder was connected to a Graham condenser (Cole-Parmer CNG200) using a rubber stopper (Figure A.2). The condenser was used to reduce the temperature of the volatile gas to provide the ideal manufacturer operating conditions for the XAD tubes (39 to 50 °C). Cooled vapors from the Graham condenser were routed through a vacuum adaptor into a PFAS emission collection to sample for: (i) targeted PFAS, (ii) suspect screening for PFAS, and (iii) fluoride ion. TC measurements were recorded using a data logger (DT9805, Data Translation Inc). The cylinder was weighed before and after loading with sand to ensure that sand was accurate for mass balance calculations.

3.3.3 PFAS Emission Collection System

A PFAS collection system was used to trap all released PFAS during heating (Figure 1). A series of XAD sorption tubes (ZST-002, Zefon International) was employed to trap the cumulative emitted hydrophobic PFAS from the sand. Each sorption tube was divided into two sections. Both sections contained pure coconut charcoal, 20/40 mesh, thermally activated at 600 °C (Figure A. 3). Following the sorption tubes, the gas emission passed through a series of three midjet impingers (CG-1820-01 Chemglass) used to measure the fraction of hydrophilic PFAS that escaped from the GAC and any fluorine ion from defluorination. The last impinger connected a vacuum pump (Zeny 3.5 CFM single-stage 5 Pa rotary vane economy vacuum pump) and flow totalizer (FMA-1608A Omega Ltd.) to the entire system (Figure A. 4). All connections between the condenser, sorption tubes, impingers, and pump were made using ¼ inch PVC vacuum tubing (Grainger, WWGG4EGU8). In each experiment, the pump-induced flowrate was adjusted, representing

approximately 5.3% of the injected air. Before each experiment, the system was leak-tested, ensuring minimal leakage.

Following each experiment, the granular activated carbon (GAC) from each sorption tube and water from the impinger was analyzed in triplicate for PFAS. The copper tubing, pipes, impingers, and condenser were rinsed before and after each experiment with basic methanol (1% w/w ammonium hydroxide), and these rinses were sent in triplicate for PFAS testing. Soluble fluoride analysis was also conducted on a 1 g subsample of the impinger water and post-treatment sand through aqueous extraction and analysis with a fluoride ion-selective electrode (IES). All glassware and cylinders were cleaned using a standard cleaning producer.

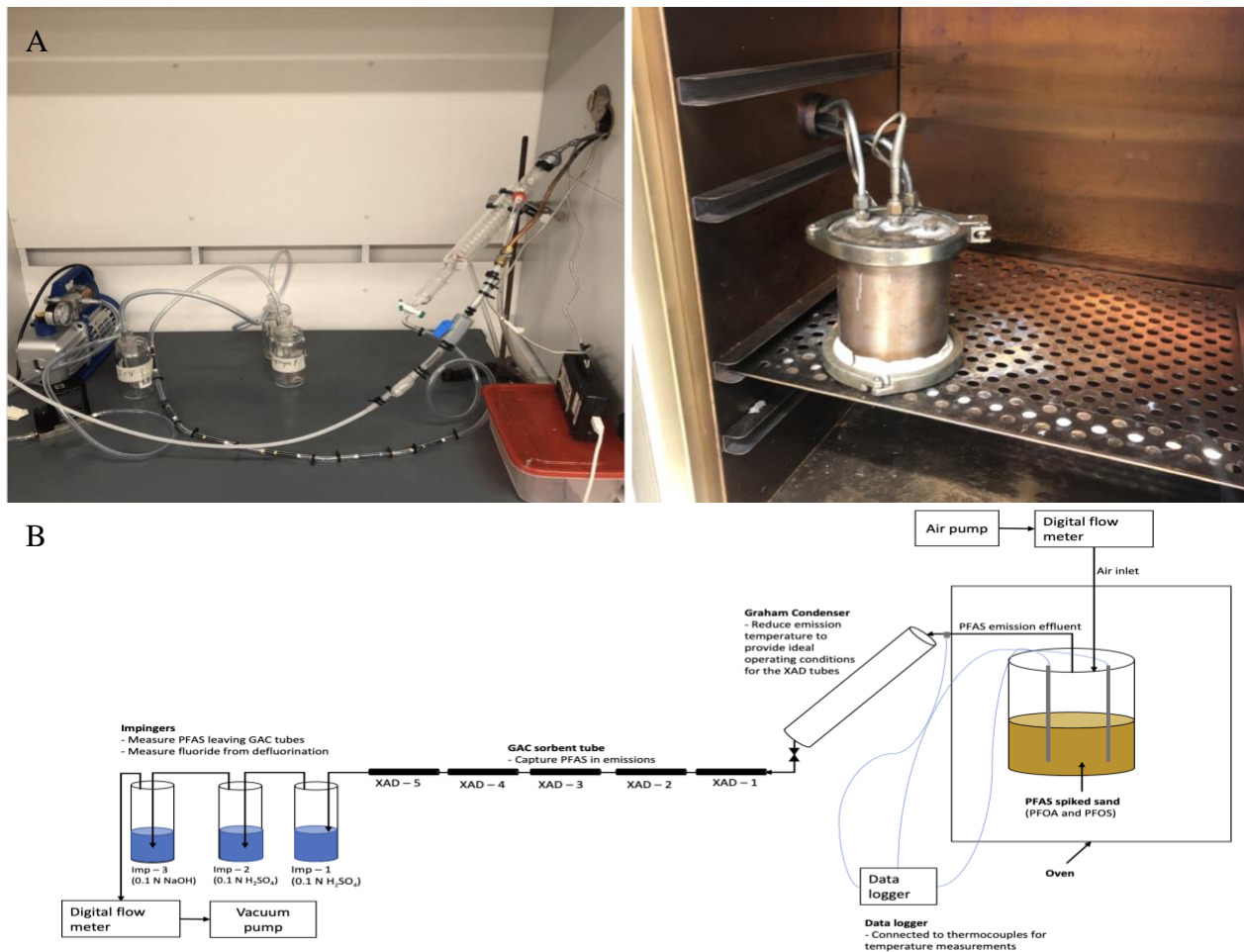


Figure 1 A) Picture of the setup showing to the right the cylinder holding the PFAS contaminated sand inside the oven, and to the left the gas capture system. B) Schematic representation of the heating and emission collection system (from right to left).

3.4 Experimental Analysis

3.4.1 PFAS Targeted Analysis

PFAS-amended solid materials (sand and GAC) were extracted using basic methanol (1% ammonium hydroxide w/w%) at a ratio of 1:10 solid/solvent with a 2-hour agitation in an end-over-end shaker at 170 rpm. Samples were centrifuged at 4000 rpm for 15 minutes, and aliquots were transferred to high-performance liquid chromatography (HPLC) vials for PFAS analysis. Liquid samples were directly subsampled into HPLC vials for analysis. Samples were diluted with basic methanol to achieve a PFAS concentration below 200 µg/L. Samples were analyzed using a Zorbax C18 Eclipse column on an Agilent 1260 HPLC coupled to an Agilent 6460 LC-MS/MS utilizing multiple-reaction monitoring (MRM) mode.

3.4.2 PFAS Suspect Screening Analysis

High concentration samples were analyzed using ddMS2 full scan mode at 60,000 resolutions in both positive and negative polarity on a ThermoFisher Exploris 120 Orbitrap coupled to a Vanquish UHPLC system using a 100 mm x 2.1 mm x 3.0 µm ACME C18 analytical column and paired guard column. The elution profile started at 90% A/10% B, transitioning to 100% B over 8 minutes, holding for 2 minutes, then equilibrating at starting conditions for 5 minutes. The potential transformation by-products were identified by subtracting chromatograms of dose 0 samples from chromatograms of dosed samples and visually inspecting the resulting chromatogram for new peaks. Where analyte intensities allowed, MS/MS data were used to confirm the transformation products identified. If possible, these products were compared to known masses of by-products in the literature.

3.4.3 Soluble Fluoride Analysis

PFAS-amended sand material was extracted using deionized water for 48 hours at a ratio of 1:4 solid/solvent with agitation using an end-over-end shaker. Liquid samples from the impingers were directly sampled without pre-treatment. Extracted solid samples were centrifuged for 20 minutes, after which 1 mL of each supernatant was transferred into a 15 mL centrifuge tube. One mL of total ionic strength adjustment buffer (TISAB) was added to the 15 mL centrifuge tube. Finally, the samples were analyzed using a fluoride ISE.

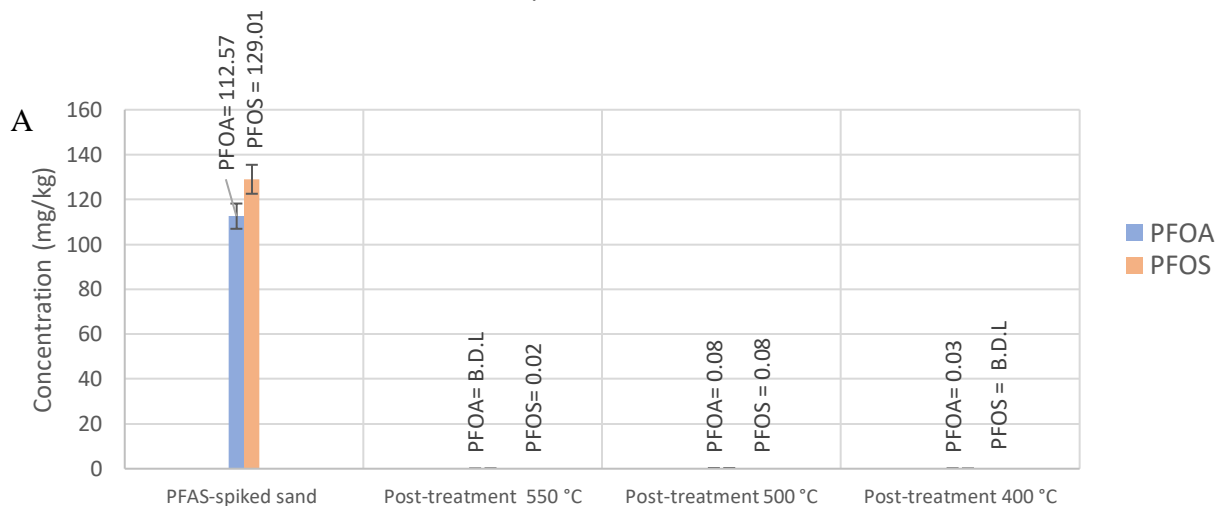
3.5 Results and Discussion

3.5.1 Experimental Phases

Experiments were conducted in two phases. Phase one explored high-temperature treatment at 550 °C, 500 °C, and 400 °C at high PFAS concentrations. The sand was spiked to create a final concentration of 112 mg PFOA/kg sand and 129 mg PFOS/kg sand. Phase two evaluated treatment at temperatures of 250 °C and 300 °C with PFAS concentrations at 25 mg PFOA/kg sand and 25 mg PFOS/kg sand to closely match the concentration profiles of some PFAS-contaminated sites [98].

3.5.2 PFAS Post-treatment Sand Removal

3.5.2.1 Phase I: Post-treatment Sand Analysis



B

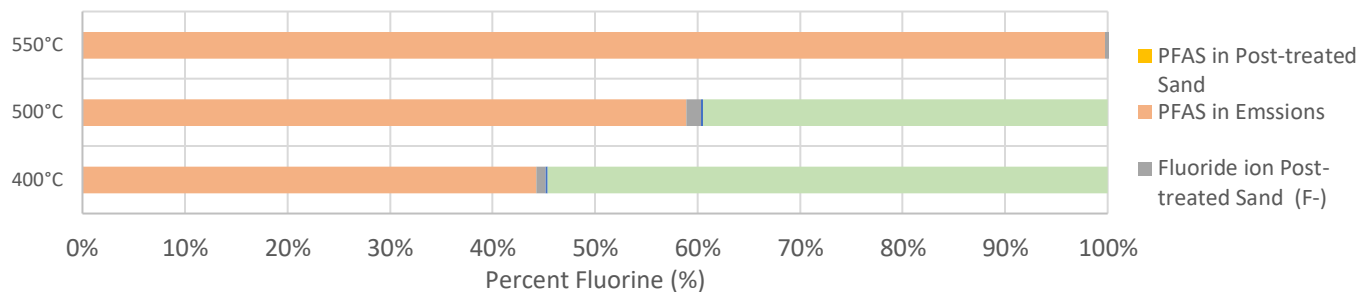


Figure 2: (A) pre-and post-treatment PFAS₁₈ concentrations for PFOS and PFOA contaminated sand (B.D.L =0.0002 mg/kg). (B) Fluorine mass balance on post-treatment experiments with spiked pre-treatment sand adjusted by the 95% of emissions that were escaped by the fume hood. Post-treatment PFAS₁₈ in the soil is plotted for all temperatures but is too small to be visible.

To study the behavior of PFAS under increasing temperature, PFAS-spiked sand was subjected to temperatures ranging from 400 °C to 550 °C for 75 minutes. This period was chosen because previous studies have shown that PFAS volatilizes between 15 and 45 minutes, and treatment times longer than 75 minutes will not lead to higher PFAS removal [97]. Therefore, to improve our understanding of the composition changes occurring in the sand and emission, individual tests were conducted at each target temperature for 75 minutes.

Figure 2.A shows that the pretreated PFAS concentrations for the spiked laboratory-created sand at 550°C, 500°C, and 400°C were 112 mg PFOA/kg sand and 129 mg PFOS/kg sand. At 550 °C, both PFOA and PFOS resulted in > 99.99% removal efficiency. Decreasing the temperature to 500 °C resulted in 99.99% and 99.93% removal efficiency of PFOA and PFOS, respectively. PFAS reduction detected in sand samples heated to 400 °C for 75 minutes resulted in 99.97% and > 99.99% removal efficiency of PFOA and PFOS, respectively.

These experiments showed that PFOA and PFOS could be removed below the detection limit at any temperature above 400°C, even at high PFAS concentrations [99] [100] [24]. Traces of long-chain PFAS (> C₈) was present in the untreated sand, likely derived from impurities in the stock solutions,

as the only PFAS compounds used in the study were PFOA and PFOS (more details in Appendix F: **PFOA and PFOS Pre- and Post-treatment Concentrations**).

The mass balance was plotted with all the reliable quantified data for the experiments with spiked pre-treatment PFAS. It includes residual PFAS₁₈ in the post-treated sand and emissions. It also contains fluoride detected in the impingers and post-treated sand that can result from PFAS defluorination (Figure 2.B).

5.2% of the emissions were sent to the emission collection system to quantify the varying PFAS in the gaseous emissions, with the remaining vented to the fume hood. Overall mass balance calculations are based on the quantitative data from the emissions capture system with the assumption that the PFAS emissions vented to the fume hood would be of a similar qualitative and quantitative composition.

PFAS heated at 550 °C in the presence of air resulted in almost complete fluorine recovery. Most of the fluorine recovered came from the emissions. This result shows that PFAS are highly resistant to mineralization even at 550 °C. This suggests that such temperatures are sufficient for volatilizing and thermally degrading PFAS to smaller chains but not enough to cause complete defluorination. At 500 °C, only 60% of the initial fluorine was recovered the majority coming from PFAS in the emission. At 400 °C, 45 % of the fluoride was recovered from PFAS in the emissions, with 2% resulting from fluoride in the impinger and post-treated sand. This study shows that heating PFAS in an oven between 400 °C and 550 °C can achieve volatilization but cannot destroy the compound. In addition, as temperature increases, more PFAS is being transformed and desorbed from the sand into the emissions.

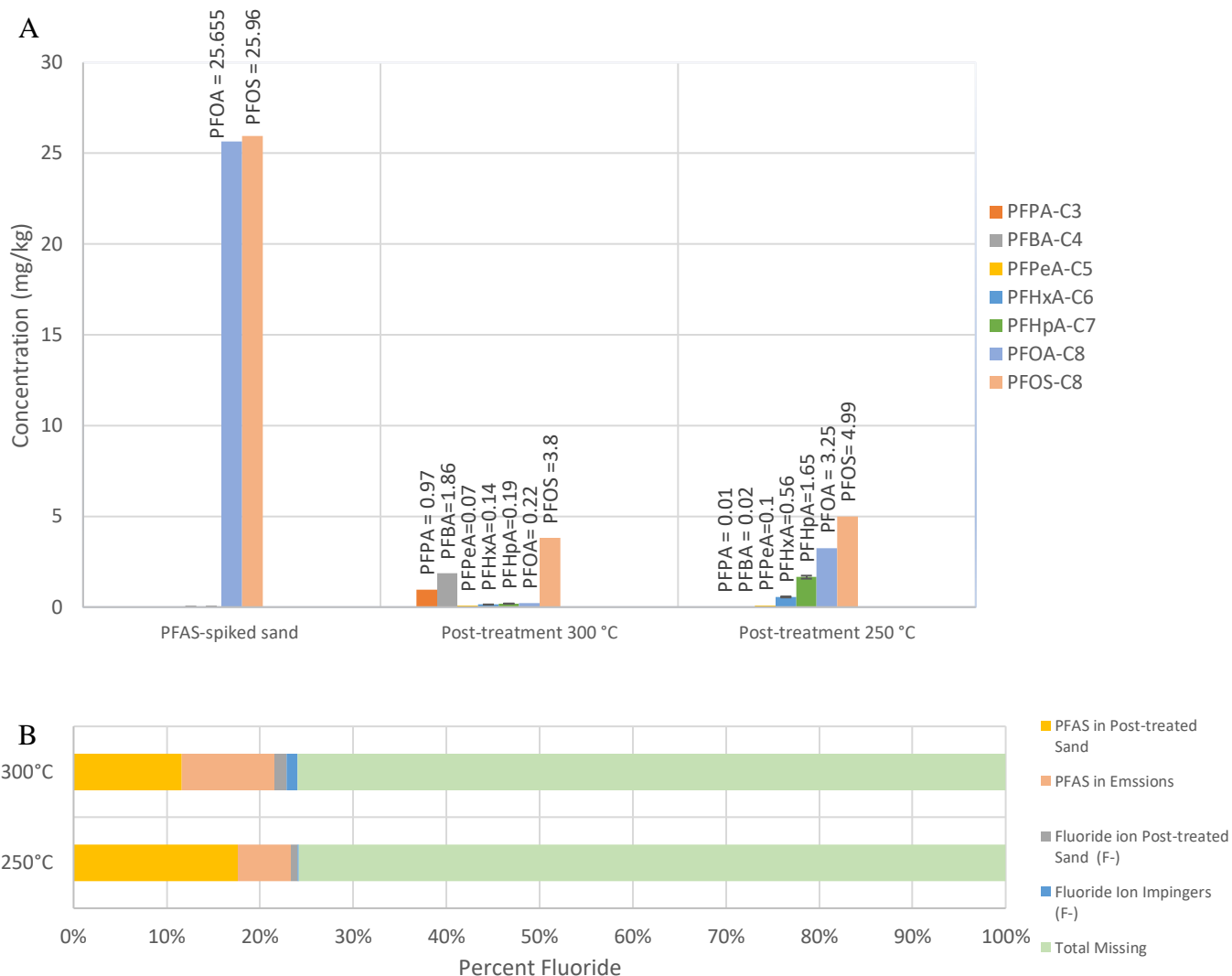


Figure 3: (A) pre-and post-treatment PFAS₁₈ concentrations for PFOS- and PFOA contaminated sand (B.D.L = 0.0002 mg/kg) at 250 °C and 300°C (B) Fluorine mass balance on post-treatment experiments with spiked pre-treatment sand.

While treatments at high temperatures can reduce PFAS concentration even at high contamination levels (>200 ppm), lower temperature remediation may have substantial cost savings. Therefore, additional testing was performed at 300 °C and 250 °C. For these tests, the sand was spiked to 25 mg PFOA/kg sand and 25 mg PFOS/kg sand to closely match some PFAS concentrations in the field. Heating PFAS-contaminated sand samples to 300 °C and 250 °C for a hold time of 75 minutes resulted in PFOA and PFOS remaining above regulatory guidelines (Figure 3.A).

At 300 °C, PFOA and PFOS achieved a removal efficiency up to 98.9% and 83.593%, respectively. Whereas at 250 °C PFOA reached 87% removal efficiency, and PFOS was approximately 83%. The lower desorption potential of PFOS than PFOA at 300 °C and 250 °C indicates that the functional group is an important factor influencing the desorption potential of PFAS. This observation demonstrates that PFSA is more strongly sorbed to sediments than PFCA, causing the lower desorption potential of PFOS [101] [102]. In addition, this data matches the reported boiling points of sulfonate-based vs. carboxylate-based PFAS, as sulfonate-based PFAS exhibit higher boiling temperatures [17].

At 300 °C and 250 °C shorter chain PFCAs such as PFBA, PFPA, PFPeA, PFHxA, and PFHpA showed PFAS generation (i.e., negative removal). This might be explained by the presence of unidentified precursors in the pretreated sand that can degrade into PFCAs [103] [104], another reason could be that these temperatures were high enough to transform PFOA and PFOS into shorter chain PFCAs but were not enough to desorb them from the sand matrix. This is a concern as shorter chain PFAS usage has increased since the ban on C₈-based PFAS. PFUnDA (C₁₁) was detected in the pretreated sand at 250 °C and 300 °C, originating from impurities in the stock solution. These results are consistent with previously published data demonstrating that 350 °C is the minimum temperature required to remediate PFAS to acceptable levels [97].

Figure 3.B shows that at 300 °C and 250 °C, 24% the fluoride was recovered. Most of the fluoride recovered at 300 °C, and 250 °C was found in the post-treatment sand coming from PFOA and PFOS in their unaltered form. A considerable extent of captured but unquantified fluoride was missing despite extensive efforts to account for all the emissions. For future studies, additional testing for total organic fluorine (TOF) and volatile organic fluoride (VOF) may be helpful to complete the mass balance.

3.5.3 PFAS GAC Breakthrough and Distribution in the Impingers

The emission gas capture line for the experiments was divided into two sections. The first section included five sorption tubes, and the second section three impingers, all connected in series. Figure 4 shows the distribution of the PFAS released by the sand in the two gas capture sections. At 550 °C, 500 °C, 400 °C, and 250 °C, the majority of the PFAS (> 94%) released were captured by the sorption tubes. Traces of PFAS were trapped by the second section of the emission train (i.e., impingers), providing evidence that very few PFAS breakthroughs occurred from the XAD tubes. However, at 300 °C, 78% of the PFAS was found in the impinger. The breakthrough was due to possible leakage in the emission train.

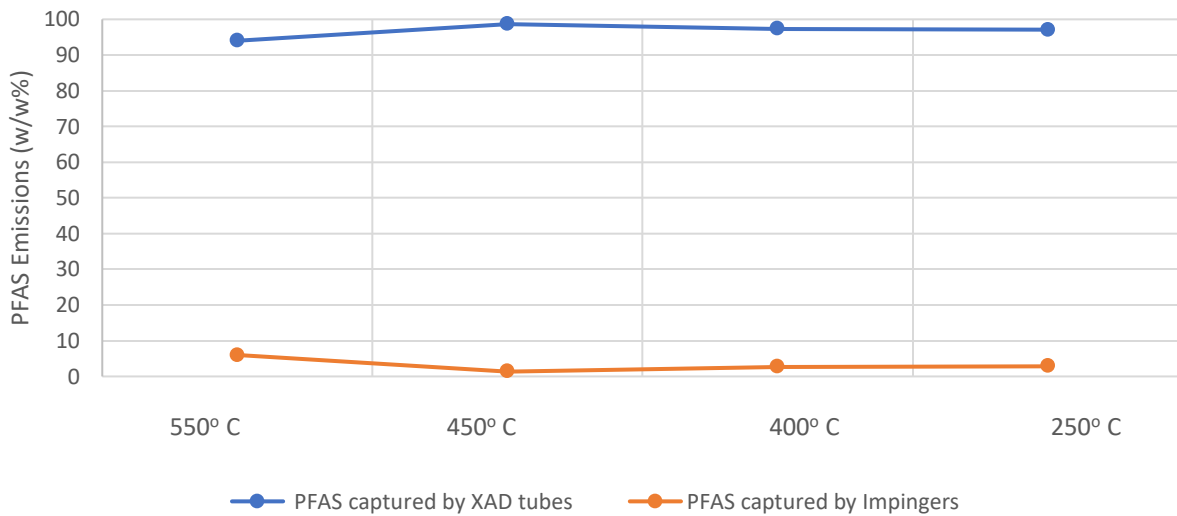


Figure 4: Percentage of PFAS captured by the XAD vs. Impinger in the emission line

3.5.4 PFAS Distribution in Different Heat Sinks

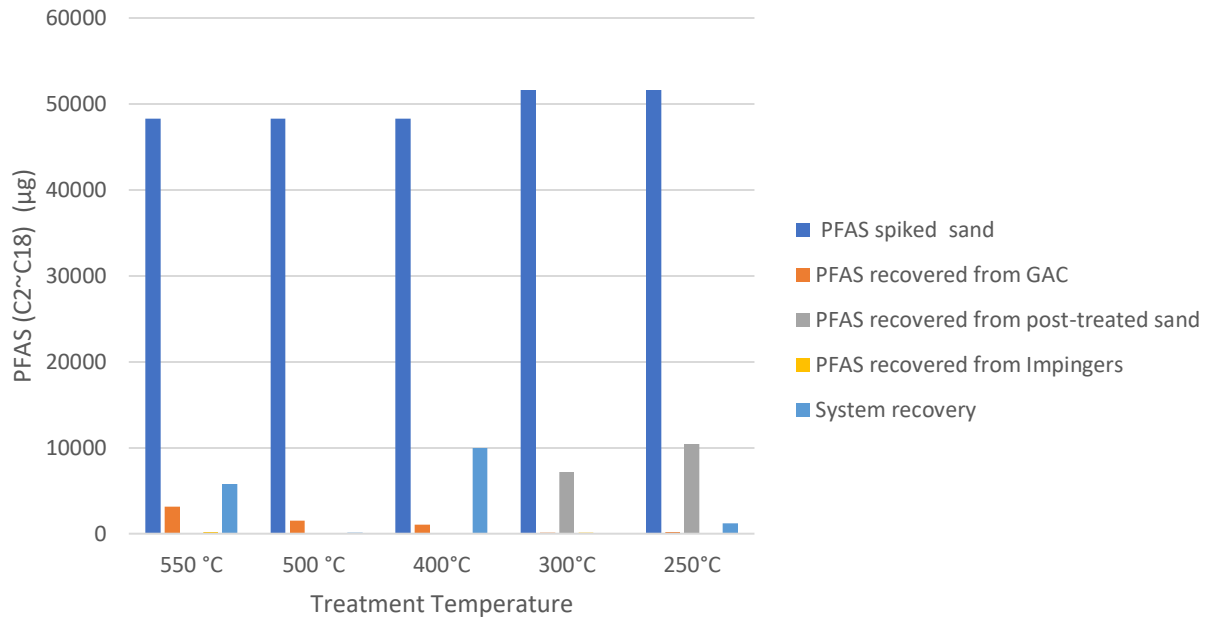


Figure 5: PFAS recovered after thermal treatment at 550 °C, 500 °C, and 400 °C for 75 minutes in different recovery sinks.

Figure 5 shows that heating PFAS-impacted sand samples at 550 °C for 75 minutes resulted in more PFAS getting captured by the emissions than that at 500 °C, 400 °C, 300°C, and 250°C. At 550 °C, the sorbent tubes captured almost 3179 µg of PFAS. However, at 500 °C and 400 °C, the detected PFAS in the GAC was 1540 µg and 1063 µg, respectively. If the temperature was reduced even further to 300 °C and 250 °C, the amount of PFAS captured by the GAC was decreased to 88 µg and 167 µg, respectively. This result indicates the effect of temperature on the thermal desorption of PFAS. The higher the temperature, the more PFAS released from the contaminated sand and captured by the GAC. PFAS was also recovered from the post-methanol rinse of the emission system. Previous studies have shown that substantial adsorption of PFOA was observed on tubes made from polypropylene (PP) and glass. In these experiments, all the emission pieces of equipment were rinsed with basic methanol three times. The highest PFAS recovered from the methanol extract was after treatments at 550 °C and 400 °C.

3.5.5 PFAS Emission Analysis at Different Treatment Temperatures

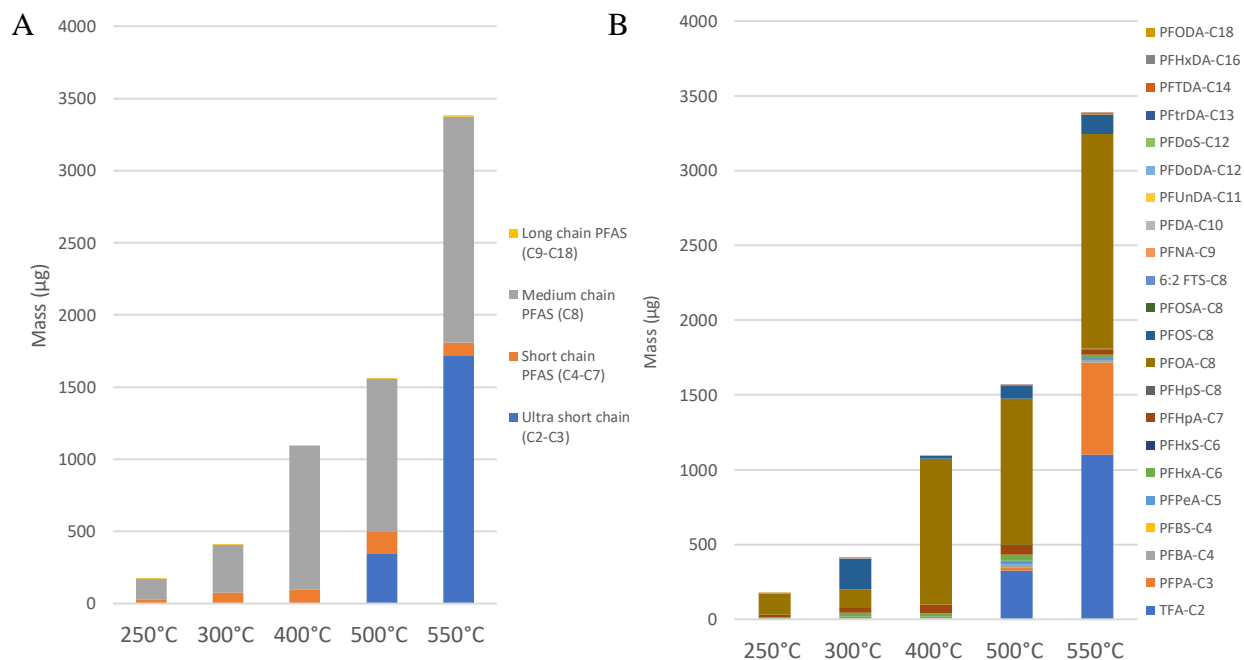


Figure 6: (A) Mass (ug) of ultra-short chain, short-chain, medium-chain, and long-chain PFAS captured by emission. (B) Mass (ug) of individual PFAS captured by the emissions. Long-chain PFAS are plotted for all temperatures but are too small to be visible.

In most experiments, shorter-chain PFAS with carboxyl and sulfonate functional groups that were not detected in the pretreated porous media mixtures were observed in the emissions. This demonstrates that PFAS heated in the sand mixture were released and transferred to the XAD tubes in substantially altered smaller-chain forms.

The highest amount of ultra-short chain PFAS captured by the emission system was at 550 °C, with 1716 µg being captured and distributed among TFA (1099 µg) and PFPA (616 µg), contributing to 50% of the emissions (Figure 6.A). At 500 °C, 347 µg of ultra-short chain PFAS were released, with 323.82 µg belonging to TFA and 23.21 µg to PFPA, representing 22% of all emissions. At 400 °C, 300°C, and 250°C, TFA and PFPA were almost absent.

C₄ to C₇ PFAS were detected at all treatment temperatures, with the majority at 500°C (150.572 µg). C₄ to C₇ PFAS show that PFOA and PFOS were transformed through +H/F⁻ exchange and dissociation of the functional group. However, unlike the previous PFAS at 550 °C, the temperature was not high enough to sustain the transformation of PFOA and PFOS down to C₂ (TFA) and C₃ (PFPA) PFAS with high masses. The majority of the C₄ to C₇ PFAS came from PFHpA, the highest being at 500°C with 67.027 µg getting captured.

The mass of all long-chain PFAS (C₉ to C₁₈) captured by the emission line at 550 °C was the highest of all treatment temperatures (approximately 6 µg). The long-chain PFAS were mainly PFDA and PFNA, with small amounts of C₁₃ and C₁₄ detected at 550 °C and 500°C. At 400°C, 300°C, and 250°C, the mass of PFNA and PFDA were lower than that at 550 °C and 500 °C, with no PFAS with carbon chain length greater than C₁₂ being detected. Even though the amount of long-chain PFAS was much less than that of shorter PFAS, it can still have environmental impacts as longer-chained PFAS tend to be more toxic and bio accumulative [105] [97] [106].

C₈ PFAS captured by the emissions increased with increasing temperature (550 °C >500 °C >400 °C >250 °C). Most of the C₈ PFAS came from PFOA and PFOS in their unaltered form. At 300 °C and 250 °C, a large mass of the initial PFOA and PFOS was still present in the post-treated sand, indicating that those temperatures can achieve limited thermal desorption.

These results show that PFHpA, PFHxA, and PFPeA (C₄ to C₇) are the main PFOA degradation products at 400 °C, 300 °C, and 250 °C, whereas TFA and PFPA are more favored at 550 °C and 500 °C. In addition, PFAS carboxylates were present (PFHpA, PFHxA, and PFPeA), but sulfonates were almost absent. Only 1.029 µg and 2.36 µg of PFHpS were found at 550 °C and 500 °C, respectively. Carboxylate versions of the sulfonates may be breakdown products (PFOS → PFOA, PFHxS → PFHxA, PFBS → PFBA). PFNA and PFDA were the most detected long-chain PFAS for all treatment temperatures. Therefore, further studies are required to study the fate of these two

PFAS during the thermal degradation of PFOA and PFOS since they might further transform into shorter chain PFAS at higher temperatures or longer residence time. The data from Figure 3 and Figure 6 show that PFOA and PFOS are always transforming, whether they are sorbed to the sand particle or suspended in the emissions. For example, experiments at 300 °C and 250 °C detected PFAS transformational products in the emissions and post-treated sands. Therefore, transformation is not just limited in the contaminated matrix, PFAS transformation can occur in the emissions released during heating (Figure 7).

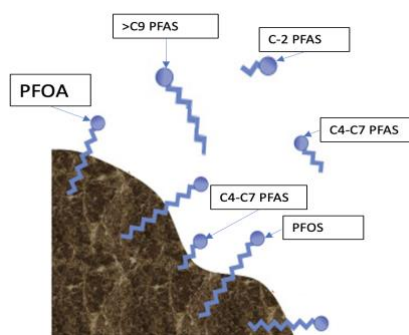


Figure 7: Schematic representation showing the transformation of PFOA and PFOS on the sand matrix and emissions

3.5.6 PFAS Transformation Products at 550°C

PFAS mass balance showed that as much as 70% to 80% of the initial amount of PFAS was missing. This result might be due to the formation of unknown organofluoride compounds from PFOA and PFOS that require greater analytical coverage. Therefore, liquid chromatography high-resolution mass spectroscopy (LC-HS-MS) was used on the first sorption tube at 550 °C since many short, and long-chain PFASs were detected.

The chromatogram of Figure 8.A shows the peak at 5.9 minutes representing Perfluorohexadecanoic acid, PFH_xDA (C₁₆). A previously constructed computational fluid dynamic combustion model developed to simulate the destruction of C₁ and C₂ PFAS revealed that

at temperatures above 930 °C, a hydrogen abstraction of a CF₃-H bond could cause the formation of the trifluoromethyl radical (CF₃·), which can undergo further reactions with other fluorinated species to form larger PFAS molecules [107]. Therefore, these data indicate that reactive PFAS radicals are not experiencing further degradation. Instead, they promote recombination with other PFAS at relatively moderate temperatures to form longer PFAS compounds.

3.5.6.1 Products of Incomplete Degradation

Unsaturated PFAS such as 4,5,6,6,7,7,8,8,8-nonafluorooct-2,4-enoic acid and 2,3,4,5,6,6,7,7,8,8,8-undecafluorooct-2,4-enoic acid (Figure 8.B and Figure 8.C) were detected in the first sorption tube. These PFOA mineralization products can result from a series of fluorine removals from the PFOA backbone, with double bonds forming to maintain overall chain stability. Both compounds are very similar, with 2,3,4,5,6,6,7,7,8,8,8-undecafluorooct-2,4-enoic acid having fluoride instead of hydrogen attached to the carbon with the double bonds. In the presence of water, these compounds should oxidize rapidly to smaller-chain PFAS, but since the GAC was extracted with methanol, no water was present to oxidize these double bonds. Intermediate products indicate that defluorination can occur on the carbon backbone and is not limited to the ionic head. However, additional studies are required to adequately describe the chemistry of all the intermediate by-products.

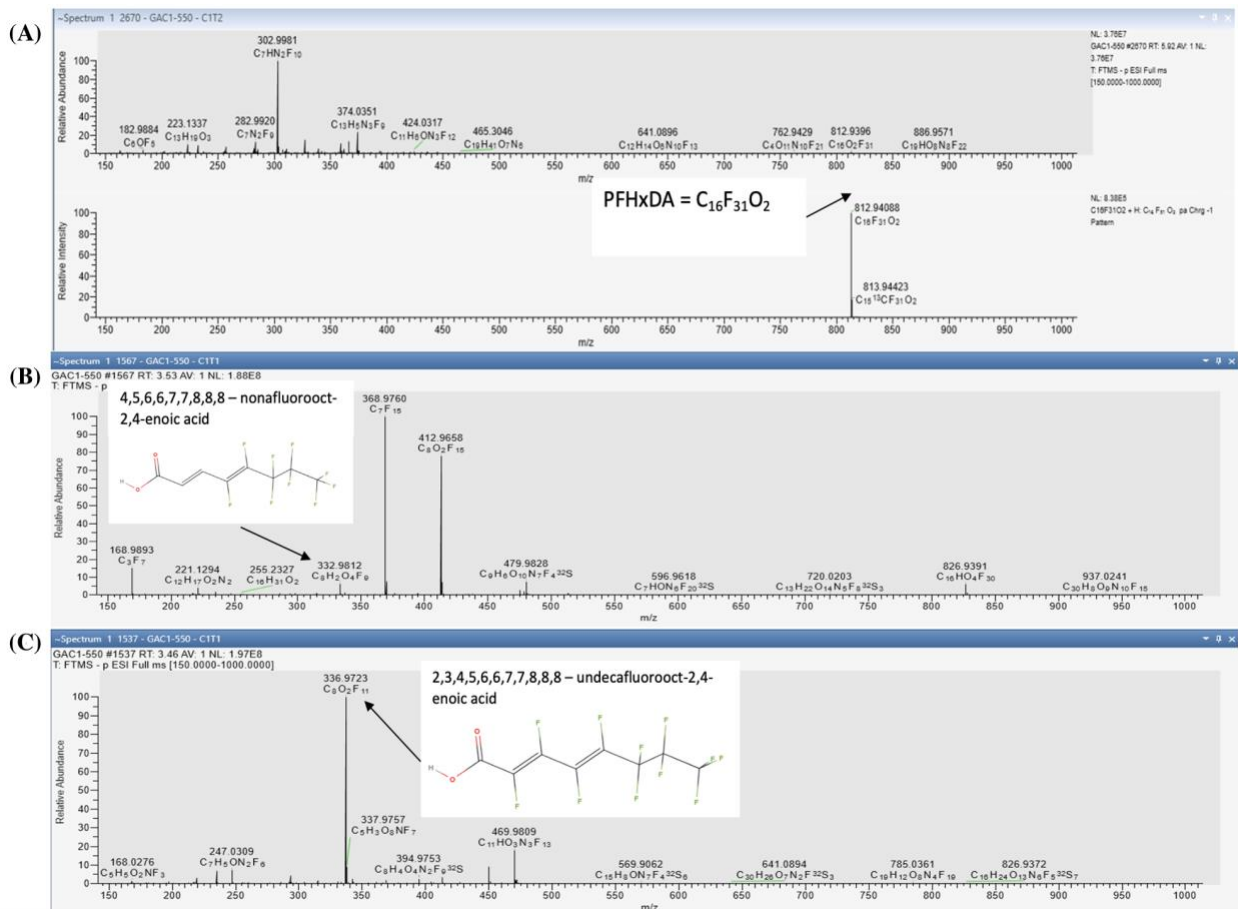


Figure 8: Full scan base peak MS chromatogram of the methanol extract of XAD-1 at 550 °C showing the presence of (A) PFHxDA, (B) 4,5,6,6,7,7,8,8,8-nonafluorooct-2,4-enoic acid, and (C) 2,3,4,5,6,6,7,7,8,8,8-undecafluorooct-2,4-enoic acid.

3.5.6.2 Perfluoroalkyl Amides (PFAAs)

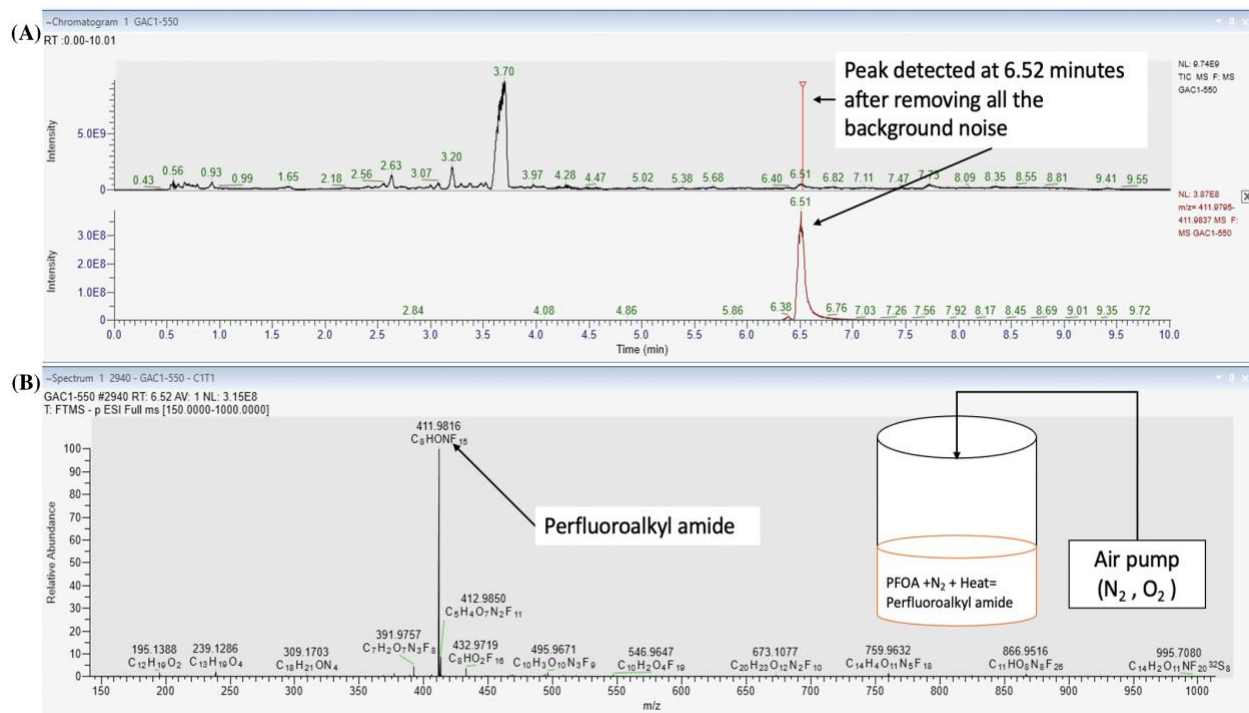


Figure 9: (A) Full scan base peak MS chromatogram of the methanol extract of XAD-1 at 550 °C shows the peak's intensity at 6.52 minutes after removing the background noise. (B) Complete scan base peak MS chromatogram of the methanol extract of XAD-1 at 550 °C, showing the relative abundance of a perfluoroalkyl amide (C_8HONF_{15}) at 6.52 minutes.

The GAC also captured many PFAS containing nitrogen. These compounds have a long carbon chain length, and it is challenging to determine which compounds are present. For example, compounds with three nitrogen atoms on the carbon chain were detected (more details in Figure K. 1). The nitrogen found in the PFAS originates from the air supplied into the cylinder. At high temperatures, oxygen atoms can attack the triple bond in N_2 , which will cause the formation of nitrogen oxide (NO_x) and nitrogen atoms (N). In addition, some hydrocarbon radicals that might be present in the system (CH_3 , CH_2 , and CH , among others) will rapidly react with nitrogen (N_2) to form NO_x or a reactive nitrogen intermediate (N_2O , cyanide, NNH) that can further oxidize into NO_x [108]. Therefore, the presence of a high amount of nitrogen oxides and free nitrogen radicals causes the formation of some of the PFAS compounds.

The chromatogram of Figure 9.A shows one large peak at 6.51 minutes after removing the background noise. This peak represents a compound with a molecular formula of C_8HONF_{15} ; considering the mass retention time, the best candidate for this compound is a perfluoroalkyl amide (PFAAms) which is very similar to PFOA except that the alcohol group has been replaced with an amine group. The chromatogram of Figure 9.B shows the relative abundance of this compound with its corresponding molecular weight, which further asserts that what we are identifying is PFAAms.

No information is found in the literature about the thermal behavior of PFAAms. However, previous results have shown that longer-chain PFAS, especially PFOA, tend to break down into reactive radicals that form short and long-chain PFAS. Therefore, PFAAms should behave in a similar pattern. Homologous series detection and high-resolution liquid chromatography-mass spectroscopy was scanning repeating units $-CF_2-$ with an amide functional group to prove the existence of a potential homologous series associated with PFAAms. The results showed C_3 amides up to C_{17} amides (Figure 10). The narrow retention time and the increasing m/z ratio further support the chemical structure. These PFAS obtained have never been reported before. These unknown PFAS suggest advancing the PFAS research beyond PFCA and PFSA and properly monitoring all emissions released during any remediation process when applicable.

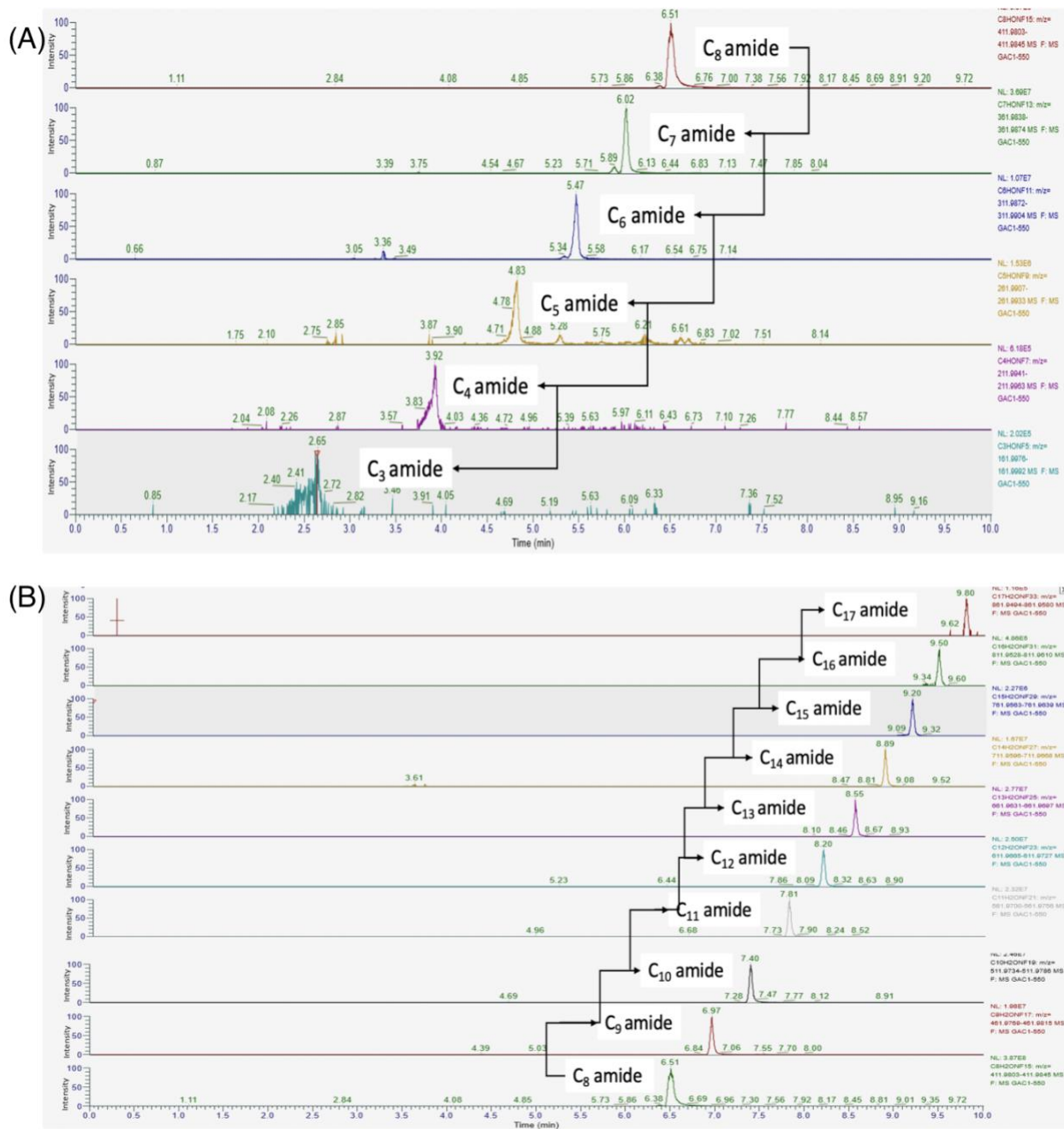


Figure 10: full-scan base peak MS chromatogram of the methanol extract of XAD-1 at 550 °C showing: (A) C₈ to C₃ amides with their corresponding intensities, (B) C₈ to C₁₇ amides with their corresponding intensities.

3.6 Summary of PFAS Recovered and Proposed Degradation and Transformation Pathways

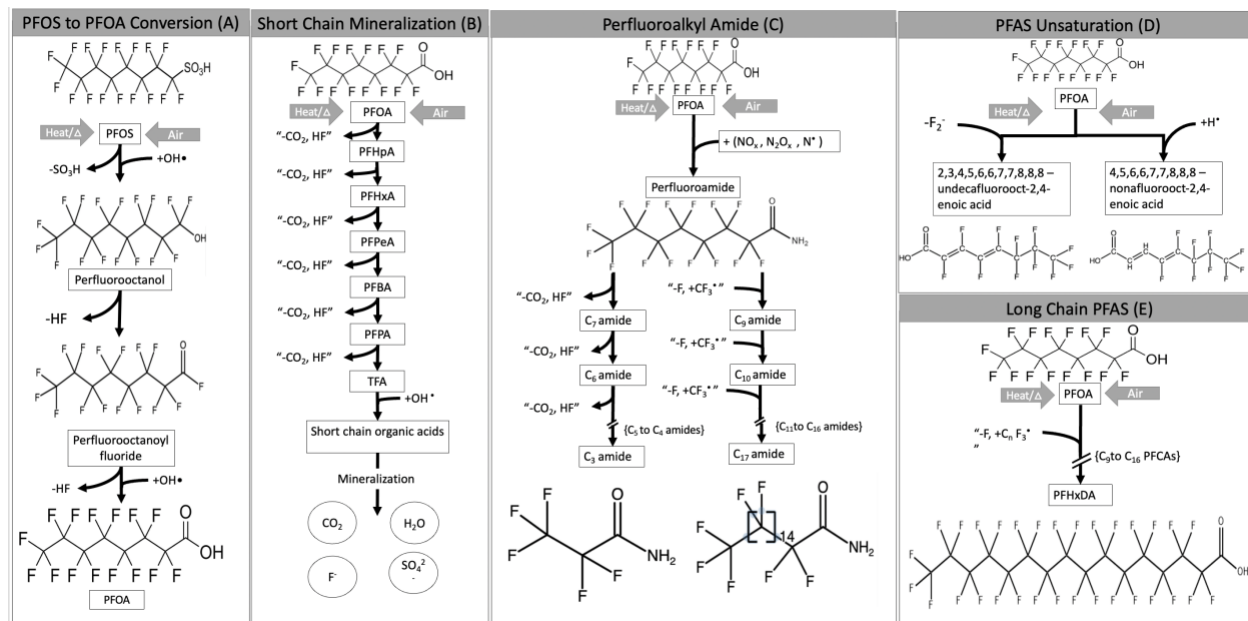


Figure 11: PFAS detected in the first sorption tube at 550°C with some of their proposed mechanisms.

The following section lists all the PFAS detected in the first sorption tube at 550°C with some of the proposed degradation pathways. Figure 11.A shows that at 550°C, PFOS will be attacked by OH• and lose a sulfonic acid (-SO₃H) to transform into perfluorooctanol, which will also lose an HF to transform into perfluorooctanoyl fluoride; the latter PFAS will get rid of an HF and get attacked by OH• to transform into PFOA

PFOA already present in the sand and that formed from PFOS will then be attacked by a H• to create unsaturated PFAS with double bonds that are highly reactive and can transform into shorter chains through the loss of HF and the release of CO₂ (Figure 11.B).

The presence of air (nitrogen and oxygen) at high temperatures will form a nitrogen complex (e.g., NO_x•, N•) that can attack PFOA to replace its functional group with an amide to form PFAAms. Like PFOA, PFAAms will develop highly reactive and unsaturated PFAAms that can transform

into short-chain PFAAs through the sequential loss of HF, and long-chain PFAAs by the addition of $\text{CF}_3\cdot$ (Figure 11.C)

Figure 10.D shows some possible structures of those highly reactive unsaturated PFAS with various double bonds on the carbon chain. These compounds are highly reactive and can oxidize rapidly in the presence of water. We suggest that some of these unsaturated PFAS are the intermediate products that allow PFOA and PFAAs to oxidize down to C_2 PFAS and are responsible for forming reactive $\text{CF}_3\cdot$ radicals that can form longer chain PFAS. Finally, figure 10.E confirms that longer chain PFAS can be formed from PFOA and PFOS reactive radicals at 550°C .

3.7 Environmental Significance

Remediation technologies are needed for treating PFAS-contaminated soil. Especially as landfilling PFAS-contaminated soils is becoming more complex and unaccepted due to increasingly prohibiting regulations. Meanwhile, in-situ thermal remediation is a viable option used with various contaminants. This study reveals that thermal remediation of PFAS-contaminated sand is an effective treatment option. Heating sand at any temperature above 400°C is expected to remove the PFAS from the soil, even at extremely high concentrations. However, it is difficult to achieve complete mineralization at temperatures below 550°C . The fraction of PFAS mineralized is less than 2%. The PFAS that is not destroyed is mainly transformed into shorter-chained PFAS and other fluorinated compounds that can be captured on GAC in the emissions. It is reasonable to suspect that the fraction of PFAS mineralized can be improved with increasing temperatures, but this approach can be cost-prohibitive. While remediation of PFAS in soil represents success, it is acknowledged that emission needs to be carefully managed and accounted for. Current thermal remediation sites should carefully monitor their emissions as some PFASs released are unknown in terms of toxicity and bioaccumulation behavior. The results of this work

showed the occurrence of perfluoroalkyl amides in the emission and provided strong evidence for the need to monitor all emissions released during any treatment process. Future work should focus on the transformation potential and toxicity of these newly detected PFAS presented in this thesis. Until further advancement in toxicological studies that can help determine whether those unknown PFAS can be discharged or not, using GAC to trap all the emissions released during heating PFAS can be an option for sites currently implementing this technology for treating soils.

Chapter 4

4.1 Conclusions

This thesis focused on laboratory studies to assess the effectiveness of in situ thermal remediation technologies on soil contaminated with PFOA and PFOS. Five studies were conducted at different temperatures to determine the ability of heat to remediate PFAS-contaminated sand at a 75-minute treatment time. The first three experiments were conducted at 550 °C, 500 °C, and 400 °C at a PFAS concentration of 200mg PFAS/kg sand. The last two experiments were conducted at temperatures 300°C and 250°C at PFAS concentrations of 50mg PFAS/kg sand. Post-treatment sampling from these experiments was used to assess the different transformation products in the sand pre-and post-treatment. A method was developed to identify and quantify, when possible, the compounds released by the emissions. This research presents a comprehensive study of fluorine mass balance under thermal remediation. The following is a list of objectives addressed during the experiments with the corresponding contributions from this work:

- 1- Objective:** Evaluate the ability of heat to remediate PFAS-contaminated sand in situ over a range of temperatures (550 °C, 500 °C, 400 °C, and 300 °C) in the presence of air.

Results: High concentrations of PFOA and PFOS were reduced to low or non-detectable values at treatment temperatures of 550 °C, 500 °C, and 400 °C. At 300 °C and 250 °C, the heat was insufficient to allow the PFAS to be removed below screening values, even at low concentrations, causing some short-chain PFAS that were not found in the pre-treated sand to be detected in the post-treated sand—proving that lower temperatures can remove the PFAS from the soils. However, temperatures above 400 °C are required to drop it below soil screening values.

- 2- Objective:** Gain knowledge about the transformation products released during the heating process by measuring a broad suite of PFAS, including PFCAs and PFSAAs.

Results: Emissions results indicated that PFAS are being transformed during thermal treatment. During thermal remediation, chain shortening, chain combination, and hydrogen/fluorine exchanges occur. The non-targeted analysis demonstrated that a wide variety of shorter-chain fluorinated products are formed during heating. The predominant PFASs released were TFA and PFPA at 500 °C and 550 °C, while at 400 °C, 300 °C, and 250 °C, PFHpA and PFHxA were the main PFASs released. PFDA and PFNA were also the primary long-chain PFASs detected in the emissions at 550 °C and 500 °C treatments.

3- Objective: Complete Fluoride mass balance to better understand PFAS fate during thermal remediation.

Results: A suite of analytical methods was implemented during heating to measure the fraction of PFAS completely mineralized and shorter/longer chain compounds that can be formed. Challenges were reported while attempting to complete the fluorine mass balance. At high temperatures >400°C, most of the fluorine recovered was from the PFAS in emissions. Around ~2% originated from soluble fluoride ions made available by PFAS defluorination.

At 300 °C and 250 °C, 13.4% and 18% of the fluoride was recovered, respectively. Most of the fluoride recovered at 300 °C, and 250 °C was found in the post-treatment sand, while less than 1% in the emission. Most fluorine ions found in the post-treated sand and emissions at 300°C and 250°C originated from PFOA as organic fluorine. Therefore, completing a fluoride mass balance was challenging. Turner et al. (2020) showed that fluoride binds to the soil and is not accessible analytically after remediation, which can result in an incomplete mass balance.

4- Objective: Track down any new classes of PFAS transformational products using advanced analytical techniques to understand better the different types of PFAS released during thermal remediation and their implication for future thermal work

Results: The results revealed previously unknown PFAS degradation products. For example, 4,5,6,6,7,7,8,8,8- nonafluorooct-2,4-enoic acids, 2,3,4,5,6,6,7,7,8,8-undecfluorooctane-2,4-enoic acid, and perfluorooctanamide homologous series were detected in the emission line in XAD₁ at 550 °C. This research shows that when PFAS-contaminated sand is exposed to high temperatures, nitrogen in the air can transform into reactive complexes that can attack PFAS to form a wide variety of products that haven't been documented before. More than 2000 PFAS compounds were detected in the emissions at 550°C, some containing more than three nitrogen atoms on the carbon chain itself, suggesting that there are additional PFAS in the soil that cannot be identified using current analytical methods until a proper understanding of the ecological behavior of those compounds' emissions released by heating PFAS should be collected and monitored.

4.2 Recommendations

This research investigated the different types of PFAS released during thermal remediation. All research for this work was done in controlled laboratory experiments. As a result, there are important questions that require additional investigation.

- PFOA and PFOS, adequate remediation temperature is above ≥ 400 °C even at high concentrations. However, a naturally contaminated site may contain many PFAS and other contaminants (organic matter) that can act as a medium for PFAS sorption. Therefore, these recommendations might need to be adjusted in field experiments.
- Continuous analysis is required to quantify and qualify the unknown and shorter-chain fluorinated compounds released during heating.
- Explore options to increase the mineralization of PFAS released in the emissions. Either by adding an extra treatment stage that can recycle heat to raise the temperature of emissions or by trapping them using granular activated carbon.

- Monitoring and carefully managing the by-products released at sites where thermal remediation is implemented. Thermal remediation should take place in a controlled environment to prevent the wet and dry deposition of PFAS vapors.
- Explore some of the toxicity and environmental behaviors of perfluoroalkyl amides.
- Use the intermediate products detected in this study to understand the mechanisms of PFAS destruction better.

Literature Cited

- [1] I. Cousins, G. G. Goldenman, D. Herzke, R. Lohmann, M. Miller, C. Ng, S. Patton, M. Scheringer, X. Trier, L. Vierke, Z. Wang and J. DeWitt, "The Concept of Essential Use for Determining When Uses of PFASs Can Be Phased Out," *Environmental Science: Processes & Impacts*, vol. 21, no. 11, pp. 1803-1815, 9 April 2019.
- [2] C. A. Moody, G. N. Hebert, S. H. Strauss and J. A. Field, "Occurrence and persistence of perfluorooctanesulfonate and other perfluorinated surfactants in groundwater at a fire-training area at Wurtsmith Air Force Base, Michigan, USAELECTRONIC Supplementary Information (ESI) available: Map of location of Wurtsmith," *Journal of Environmental Monitoring*, vol. 5, no. 2, pp. 341-345, 2003.
- [3] K. Kuroda, M. Murakami, K. Oguma, H. Takada and S. Takizawa, "Investigating sources and pathways of perfluoroalkyl acids (pfaas) in aquifers in Tokyo using multiple tracers," *Science of The Total Environment*, Vols. 488-489, pp. 51-60, 2014.
- [4] V. A. Arias Espana, M. Mallavarapu and R. Naidu, "Treatment technologies for aqueous perfluorooctanesulfonate (PFOS) and perfluorooctanoate (PFOA): A critical review with an emphasis on field testing," *Environmental Technology & Innovation*, vol. 4, pp. 168-181, 2015.
- [5] X. C. Hu, D. Q. Andrews, A. B. Lindstrom, T. A. Bruton, L. A. Schaider, P. Grandjean, R. Lohmann, C. C. Carignan, A. Blum, S. A. Balan, C. P. Higgins and E. M. Sunderland, "Detection of poly- and perfluoroalkyl substances (pfass) in U.S. drinking water linked to industrial sites, military fire training areas, and wastewater treatment plants," *Environmental Science & Technology Letters*, vol. 3, no. 10, pp. 344-350, 2016.
- [6] C. M. Teaf, M. M. Garber, D. J. Covert and B. J. Tuovila, "Perfluorooctanoic acid (PFOA): Environmental sources, chemistry, toxicology, and potential risks," *Soil and Sediment Contamination: An International Journal*, vol. 28, no. 3, pp. 258-273, 2019.
- [7] N. M. Bernnan, A. T. Evans, K. M. Fritsch, S. A. Peak and H. E. Vn Holst, "Trends in the regulation of per- and polyfluoroalkyl substances (PFAS): A scoping review," *International Journal of Environmental Research and Public Health*, vol. 8, no. 20, p. 10900, 2021.
- [8] M. Trojanowicz, A. Bojanowska-Czajka, I. Bartosiewicz and K. Kulisa, "Advanced oxidation/reduction processes treatment for aqueous perfluorooctanoate (PFOA) and perfluorooctanesulfonate (PFOS) – a review of recent advances," *Chemical Engineering Journal*, vol. 336, pp. 170-199, 2018.
- [9] N. Törneman, "Remedial methods and strategies for perfluorinated compounds," in *4 th Nordic Joint Meeting on Remediation of Contaminated Sites International Conference*, Oslo, 2012.
- [10] T. Pancras, W. Plaisier and A. Barbier, "Challenges of PFOS Remediation," in *Proceedings of the AquaConSoil Conference*, Barcelona, ES, 2013.

- [11] M. F. Kuehnel, D. Lentz and T. Barun, "Synthesis of fluorinated building blocks by transition-metal-mediated hydrodefluorination reactions," *ChemInform*, vol. 44, no. 27, 2013.
- [12] J. E. Vidonish, K. Zygourakis, C. A. Masiello, G. Sabadell and P. J. J. Alvarez, "Thermal Treatment of Hydrocarbon-Impacted Soils," *A Review of Technology Innovation for Sustainable Remediation*, vol. Engineering 2, pp. 426-437, 2016.
- [13] P. C. Higgins and G. R. Luthy, "Sorption of perfluorinated surfactants on sediments," *Environmental Science & Technology*, vol. 40, no. 23, pp. 7251-7256, 2006.
- [14] A. Leeson, H. F. Stroo and P. C. Jhonson, "Groundwater remediation today and challenges and opportunities for the future," *GroundWater*, vol. 51, pp. 175-179, 2013.
- [15] N. Watanbe, S. Takemine, K. Yamamoto, Y. Haga and M. Takata, "Residual organic fluorinated compounds from thermal treatment of PFOA, pfhxa and PFOS adsorbed onto granular activated carbon (GAC)," *Journal of Material Cycles and Waste Management*, vol. 18, no. 4, pp. 625-630, 2016.
- [16] W. Tsang, R. D. Burgess and V. Babushok, "On the incinerability of highly fluorinated organic compounds," *Combustion Science and Technology*, vol. 139, no. 1, pp. 385-402, 1998.
- [17] E. Crownover, D. Oberle, M. Kluger and G. Heron, "Perfluoroalkyl and polyfluoroalkyl substances thermal desorption evaluation," *Remediation Journal*, vol. 29, no. 4, pp. 77-81, 2019.
- [18] O. S. Arvaniti and A. S. Stasinakis, "Review on the occurrence, fate and removal of perfluorinated compounds during wastewater treatment," *Science of the Total Environment*, vol. 524, pp. 81-92, 2015.
- [19] USEPA, "Technical Fact Sheet – Perfluorooctane Sulfonate (PFOS) and Perfluorooctanoic Acid (PFOA)," USEPA, Washington, DC, 2017.
- [20] L. Ahrens, "Polyfluoroalkyl compounds in the aquatic environment : A review of their occurrence and fate," *Journal of Environmental Monitoring*, vol. 13, pp. 20-31, 2011.
- [21] D. C. Burns, D. E. A. Ellis, H. Li, C. J. McMurdo and E. Webster, "Experimental pKa determination for perfluorooctanoic acid (PFOA) and the potential impact of pKa concentration dependence on laboratory-measured partitioning phenomena and environmental modeling," *Environmental Science and Technology*, vol. 42, no. 24, pp. 9283-9288, 7 November 2008.
- [22] B. J. Place and J. A. Field, "Identification of novel fluorochemicals in aqueous film-forming foams used by the US military," *Environmental Science & Technology*, vol. 46, no. 13, pp. 7120-7127, 2012.
- [23] M. Rahman, S. Peldszus and W. Anderson, "Behaviour and fate of perfluoroalkyl and polyfluoroalkyl substances (pfass) in drinking water treatment: A Review," *Water Research*, vol. 50, pp. 318-340, 2014.

- [24] Health Canada, "Updates to Health Canada Soil Screening Values for Perfluoroalkylated Substances (PFAS)," 2019.
- [25] N. Wang, J. Liu, R. Bucl, S. Korzeniowski, B. Wolstnholme, P. Folsom and L. Sulecki, "6:2 Fluorotelomer sulfonate aerobic biotransformation in activated sludge of waste water treatment plants," *Chemosphere*, vol. 82, no. 6, pp. 853-858, 2011.
- [26] Z. Zhou, Y. Liang, Y. Shi, L. Xu and Y. Cai, "Occurrence and Transport of Perfluoroalkyl Acids (PFAAs), Including Short-Chain PFAAs in Tangxun Lake, China," *Environmental Science & Technology*, vol. 47, no. 16, pp. 9249-9257, 2013.
- [27] J.-W. Kim, N. M. Tue, T. Isobe, K. Misaki, S. Takahashi, P. Viet and S. Tanabe, "Contamination by perfluorinated compounds in water near waste recycling and disposal sites in Vietnam," *Environmental Monitoring and Assessment*, vol. 185, no. 4, pp. 2909-2919, 2012.
- [28] S. Castiglioni, S. Valsecchi, S. Polesello, M. Rusconi, M. Melis, M. Palmiotto, A. Manenti, E. Davoli and E. Zuccato, "Sources and fate of perfluorinated compounds in the aqueous environment and in drinking water of a highly urbanized and industrialized area in Italy," *Journal of Hazardous Materials*, vol. 282, pp. 51-6, 2015.
- [29] A. Becker, S. Gerstmann and H. Frank, "Perfluorooctanoic acid and perfluorooctane sulfonate in the sediment of the Roter Main river, Bayreuth, Germany," *Environmental Pollution*, vol. 156, no. 3, pp. 818-820, 2008.
- [30] M. Kotthoff, J. Muller, H. Jurling, M. Sclumer and D. Fiedler, "Perfluoroalkyl and polyfluoroalkyl substances in consumer products," *Environmental Science and Pollution Research*, vol. 22, no. 19, pp. 14546-14559, 2015.
- [31] T. Anumol, S. Dagnino, D. R. Vandervort and S. A. Synder, "Transformation of Polyfluorinated compounds in natural waters by advanced oxidation processes," *Chemosphere*, vol. 144, pp. 1780-1787, 2016.
- [32] L. Zhao, P. W. Folsom, B. W. Wolstnholme, H. Sun, N. Wang and R. Buck, "6:2 Fluorotelomer alcohol biotransformation in an aerobic river sediment system," *Chemosphere*, vol. 90, no. 2, pp. 203-209, 2013.
- [33] M. H. Kim, N. Wang, T. McDonald and K.-H. Chu, "Biodefluorination and biotransformation of fluorotelomer alcohols by two alkane-degrading *Pseudomonas* strains," *Biotechnology and Bioengineering*, vol. 109, no. 12, pp. 3041-3048, 2012.
- [34] S. Zhao and L. Zhu, "Uptake and metabolism of 10:2 fluorotelomer alcohol in soil-earthworm (*Eisenia fetida*) and soil-wheat (*triticum aestivum* L.) systems," *Environmental Pollution*, vol. 220, pp. 123-131, 2017.

- [35] F. E. Houtz, R. Sutton, J.-S. Park and M. Sedlak, "Poly- and PERFLUOROALKYL substances in WASTEWATER: Significance of unknown precursors, MANUFACTURING shifts, and likely Afff impacts," *Water Research*, vol. 95, pp. 142-149, 2016.
- [36] C. S. Panel, "Probable link evaluation of thyriod diseases," 30 July 2012. [Online]. Available: http://www.c8sciencepanel.org/pdfs/Probable_Link_C8_Cancer_16April2012_v2.pdf. [Accessed 23 05 2021].
- [37] E. Bonefeld-Jorgensen, M. Long and R. Bossi, "Prfluorinated compounds are related to breast cancer risk in Greenlan Inuit: A case control study," *Environ. Health*, vol. 10, p. 88, 2011.
- [38] S. C. Chang, K. Das, D. J. Ehresam, M. E. Ellefson, G. Gorman, J. A. Hart, P. E. Noker, T. Yu-Mei, P. H. Lieder, C. Lau, G. W. Olsen and J. L. Butenhoff, "Comparative pharmacokinetics of perfluorobutyrate in rats, mice, monkeys, and humans and relevance to human exposure via drinking water," *Toxicological Sciences*, vol. 104, no. 1, pp. 40 - 53, 2008.
- [39] H. Zhu and K. Kannan, "Distribution and partitioning of perfluoroalky carboxylic acids in surface soil, plants, and earthworms at a contaminated site," *Science of Total Environment*, vol. 647, p. 9540961, 2019.
- [40] R. L. Johnson, A. J. Anschutz, J. Smolen, S. M. F. and R. L. Penn, "The adsorption of perfluorooctane sulfonate onto, sand, clay, and iron oxide surfaces," *J. Chem. Eng. Data*, vol. 52, pp. 1165-1170, 2007.
- [41] W. Zongsu, T. Xu and D. Zhao, "Treatment of per-and polyfluoroalkyl substances in landfill leachate: status, chemistry and prospect," *Environmental Science Water Research Technology*, vol. 5, pp. 1814-1835, 2019.
- [42] R. Darlington and E. M. J. Barth, "The challenges of PFAS Remediation," *The Military engineer*, vol. 110, no. 712, pp. 58-60, 2018.
- [43] I. Ross, J. McDonough, J. Miles, P. Storch, P. T. Kochunarayana, E. Klave, J. Hurst, S. S. Dagupta and J. Burdick, "A review of emerging technologies for remediation of PFASs," *Remediation Journal*, vol. 28, pp. 101-126, 2018.
- [44] H. A. V. Hellsing S. Josefsson and L. Ahrens, "Sorption of perfluoroalky substances to two types of minerals," *Remediation Journal*, vol. 9, pp. 65-72, 1999.
- [45] Y.-C. Chen, S.-L. Lo, N.-H. Li, Y.-C. Lee and J. Kuo, "Sorption of perfluoroalkyl substances (PFASs) onto wetland soils," *Desalination and Water Treatment*, vol. 51, no. 40-42, pp. 7469-7475, 2013.
- [46] H. Chen, S. Chen, X. Quan, Y. Zhao and H. Zhao, "Sorption of perfluorooctane sulfonate (PFOS) on oil and oil-derived black carbon: Influence of solution pH and [Ca²⁺]," *Chemosphere*, vol. 77, no. 10, pp. 1406-1411, 2009.

- [47] Y. Li, D. P. Oliver and R. S. Kookana, "A critical analysis of published data to discern the role of soil and sediment properties in determining sorption of per and polyfluoroalkyl substances (PFASs)," *Science of the Total Environment*, Vols. 628-629, pp. 110-120, 2018.
- [48] C. Y. Tang, S. Q. Fu, D. Gao, C. S. Criddle and J. O. Leckie, "Effect of solution chemistry on the adsorption of perfluorooctane sulfonate onto mineral surfaces," *Water Research*, vol. 44, no. 8, pp. 2654-2662, 2010.
- [49] L. Zhao, L. Zhu, L. Yang, L. Zhengtao and Y. Zhang, "Distribution and desorption of perfluorinated compounds in fractional sediments," *Chemosphere*, vol. 88, pp. 1390-1397, 2012.
- [50] V. Gellrich and T. P. Knepper, "The Handbook of Environmental Chemistry," in *Polyfluorinated chemicals and transformation products*, Berlin, Springer Berlin, 2013, pp. 63-72.
- [51] V. Gellrich, T. Stahl and T. P. Knepper, "Behavior of perfluorinated compounds in soils during leaching experiments," *Chemosphere*, vol. 87, no. 9, pp. 1052-1056, 2012.
- [52] L. J. Guelfo and P. C. Higgins, "Subsurface transport potential of perfluoroalkyl acids at aqueous film-forming foam (aFFF)-impacted sites," *Environmental Science & Technology*, vol. 47, no. 9, pp. 4164-4171, 2013.
- [53] R. Mahinroosta and L. Senevirathna, "A review of the emerging treatment technologies for PFAS contaminated soils," *Journal of Environmental Management*, vol. 255, no. 109896, pp. 1-12, 2020.
- [54] X. Chen, X. Xia, X. Wang, J. Qiao and C. Huiting, "A comparative study on sorption of perfluorooctane sulfonate (PFOS) by chars, ash and carbon nanotubes," *Chemosphere*, vol. 83, no. 10, pp. 1313-1319, 2011.
- [55] B. Sarkar, Y. Xi, M. Megharaj, G. Krishnamurti, M. Browman, R. Harry and R. Naidu, "Bioreactive Organoclay: A New Technology for Environmental Remediation," *Critical Reviews in Environmental Science and Technology*, vol. 42, no. 5, pp. 435-488, 2012.
- [56] P. Das, V. A. Arias E., V. Kambala, M. Mallavarapu and R. Naidu, "Remediation of perfluorooctane sulfonate in contaminated soils by modified clay adsorbent—a risk-based approach," *Water, Air, & Soil Pollution*, vol. 224, no. 12, 2013.
- [57] Y. H. Aly, D. P. McInnis, S. M. Lombardo, A. W. A., K. D. Pennell, J. Hatton and M. F. Simcik, "Enhanced adsorption of perfluoro alkyl substances for in situ remediation," *Environmental Science: Water Research & Technology*, vol. 5, no. 11, 2019.
- [58] D. Zhao, J. Cheng, C. D. Vecitis and M. R. Hoffmann, "Sorption of Perfluorochemicals to Granular Activated Carbon in the Presence of Ultrasound," *The Journal of Physical Chemistry A*, vol. 115, no. 11, pp. 2250-2257, 2011.
- [59] Z. Du, S. Deng, Y. Bei, Q. Huang, B. Wang, J. Huang and G. Yu, "Adsorption behavior and mechanism of perfluorinated compounds on various adsorbents—A review," *Journal of Hazardous Materials*, vol. 274, pp. 443-454, 2014.

- [60] D. B. V, R. K. R, P. David and K. Weber, "PFOA and PFOS diffusion through LLDPE and Lldpe coextruded with EVOH at 22 °C, 35 °C, and 50 °C," *Waste Management*, vol. 117, pp. 93-103, 2020.
- [61] T.-T. Wang, G.-G. Ying, L.-Y. He, Y.-S. Liu and J.-L. Zhao, "Uptake mechanism, subcellular distribution, and uptake process of perfluorooctanoic acid and perfluorooctane sulfonic acid by wetland plant *Alisma orientale*," *Science of The Total Environment*, vol. 733, p. 139383, 2020.
- [62] B. Wen, L. Li, Y. Liu, H. Zhang, X. Hu, X.-q. Shan and S. Zhang, "Mechanistic studies of perfluorooctane sulfonate, perfluorooctanoic acid uptake by maize (*Zea mays* L. cv. TY2)," *Plant and Soil*, vol. 370, no. 1-2, pp. 345-354, 2013.
- [63] L. Lesmeister, F. T. Lange, J. Breuer, A. Biegel-Engler, E. Giese and M. Scheurer, "Extending the knowledge about PFAS bioaccumulation factors for agricultural plants – A review," *Science of The Total Environment*, vol. 766, p. 142640, 2021.
- [64] Z. Lan, M. Zhou, Y. Yao and H. Sun, "Plant uptake and translocation of perfluoroalkyl acids in a wheat–soil system," *Environmental Science and Pollution Research*, vol. 25, pp. 30907-30916, 2018.
- [65] D. K. Huff, L. A. Morris, L. Sutter, J. Costanza and K. D. Pennell, "Accumulation of six PFAS compounds by woody and herbaceous plants: potential for phytoextraction," *International Journal of Phytoremediation*, vol. 22, no. 14, pp. 1538-1550, 2020.
- [66] L. Gobelius, J. Lewis and L. Ahrens, "Plant Uptake of Per- and Polyfluoroalkyl Substances at a Contaminated Fire Training Facility to Evaluate the Phytoremediation Potential of Various Plant Species," *Environmental Science & Technology*, vol. 51, no. 21, pp. 12602-12610, 2017.
- [67] M. Brusseau, H. R. Anderson and B. Guo, "Pfas concentrations in soils: Background levels versus contaminated sites," *Science of The Total Environment*, vol. 740, p. 140017, 2020.
- [68] F. I. Khan, T. Husain and R. Hejazi, "An Overview and Analysis of Site Remediation Technologies," *Journal of Environmental Management*, vol. 71, pp. 95-122, 2004.
- [69] M. Wilhelm, M. Kraft, K. Rauchfuss and J. Hölzer, "Assessment and management of the First German case of a contamination WITH Perfluorinated Compounds (PFC) in the Region Sauerland, North Rhine-Westphalia," *Journal of Toxicology and Environmental Health, Part A*, vol. 71, no. 11-12, pp. 725-733, 2008.
- [70] L. Paterson, T. S. Kennedy and D. Sweeney, "Remediation of Perfluorinated Alkyl Compounds at a Former Fire Fighting Training Area," in *Proceedings of the Remediation Technologies Symposium*, Banff, AB, 2008.
- [71] J. W. Jawitz, R. K. Sillan, M. D. Annable, S. P. Rao and K. Warner, "In-Situ Alcohol Flushing of a DNAPL Source Zone at a Dry Cleaner Site," *Environmental Science & Technology*, vol. 34, no. 17, pp. 3722-3729, 2000.

- [72] G. Pan, C. Jia, D. Zhao, C. You, H. Chen and G. Jiang, "Effect of cationic and anionic surfactants on the sorption and desorption of perfluorooctane sulfonate (PFOS) on natural sediments," *Environmental Pollution*, vol. 157, no. 1, pp. 325-330, 2009.
- [73] H. F. Schröder, "Determination of fluorinated surfactants and their metabolites in sewage sludge samples by liquid chromatography with mass spectrometry and tandem mass spectrometry after pressurised liquid extraction and separation on fluorine-modified reversed-phase sor," *Journal of Chromatography A*, vol. 1020, no. 1, pp. 131-151, 2003.
- [74] L. Pasquini, C. Merlin, L. Hassnboehler, J.-F. Munoz, M.-N. Pons and T. Görner, "Impact of certain household micropollutants on bacterial behavior. Toxicity tests/study of extracellular polymeric substances in sludge," *Science of The Total Environment*, Vols. 463-464, pp. 355-365, 2013.
- [75] S. Huang and P. R. Jaffe, "Defluorination of Perfluorooctanoic Acid (PFOA) and Perfluorooctane Sulfonate (PFOS) by *Acidimicrobium* sp. Strain A6," *Environmental Science & Technology*, vol. 53, no. 19, pp. 11410-11419, 2019.
- [76] S. Chetverikov, D. Sharipov, K. T and O. Loginov, "Degradation of perfluorooctanyl sulfonate by strain *Pseudomonas plecoglossicida* 2.4-D," *Applied Biochemistry and Microbiology*, vol. 53, no. 5, pp. 533-538, 2017.
- [77] G. Kwon, H.-J. Lim, S.-H. Na, B.-I. Choi, D.-S. Shin and S.-Y. Chung, "Biodegradation of perfluorooctanesulfonate (PFOS) as an emerging contaminant," *Chemosphere*, vol. 109, pp. 221-225, 2014.
- [78] S. Mejia-Avenidaño, S. Vo Duy, S. Sauvé and J. Liu, "Generation of Perfluoroalkyl Acids from Aerobic Biotransformation of Quaternary Ammonium Polyfluoroalkyl Surfactants," *Environmental Science & Technology*, vol. 50, no. 18, pp. 9923-9932, 2016.
- [79] H. Lin, J. Niu, S. Ding and L. Zhang, "Electrochemical degradation of perfluorooctanoic acid (PFOA) by Ti/SnO₂-Sb, Ti/SnO₂-Sb/PbO₂ and Ti/SnO₂-Sb/MnO₂ anodes," *Water Research*, vol. 46, no. 7, pp. 2281-2289, 2012.
- [80] A. Tsitonakil, B. Petri, M. Crimi, H. Mosbaek, L. R. Siegrist and P. L. BJERG, "In situ Chemical oxidation of contaminated soil and GROUNDWATER Using Persulfate: A review," *Critical Reviews in Environmental Science and Technology*, vol. 40, no. 1, pp. 55-91, 2010.
- [81] J. R. Watts and L. A. Teel, "Treatment of contaminated soils and GROUNDWATER Using ISCO," *Practice Periodical of Hazardous, Toxic, and Radioactive Waste Management*, vol. 10, no. 1, pp. 2-9, 2006.
- [82] H. Hori, Y. Nagaoka, M. Murayama and S. Kustsuna, "Efficient decomposition of perfluorocarboxylic acids and alternative fluorochemical surfactants in hot water," *Environmental Science & Technology*, vol. 42, no. 19, pp. 7438-7443, 2008.
- [83] D. Patch, N. O'Connor, I. Koch, T. Cresswell, C. Hughes, J. Davies, J. Scott, D. O'Carroll and K. Weber, "Elucidating degradation mechanisms for a range of per- and polyfluoroalkyl substances

- (PFAS) via controlled irradiation studies," *Science of The Total Environment*, vol. 832, p. 154941, 2022.
- [84] G. Cagnetta, J. Robertson, J. Huang, K. Zhang and G. Yu, "Mechanochemical destruction of halogenated organic pollutants: A critical review," *Journal of Hazardous Materials*, vol. 313, pp. 85-102, 2016.
- [85] G. Cagnetta, Q. Zhang, J. Huang, M. Lu, B. Wang, Y. Wang, S. Deng and G. Yu, "Mechanochemical destruction of perfluorinated pollutants and mechanosynthesis of lanthanum oxyfluoride: A Waste-to-Materials process," *Chemical Engineering Journal*, vol. 316, pp. 1078-1090, 2017.
- [86] L. P. Turner, B. H. Kueper, K. M. jaansalu, D. Patch, N. Battye, O. El-Sharnouby, K. G. Mumford and K. P. Weber, "Mechanochemical remediation of perfluorooctanesulfonic acid (PFOS) and perfluorooctanoic acid (PFOA) amended sand and aqueous film-forming foam (AFFF) impacted soil by planetary ball milling," *Science of the Total Enviroment*, vol. 765, no. 15, p. 142722, 2021.
- [87] N. Battye, D. Patch, D. Roberts, O. Natalia, L. Turner, B. Kueper, M. Hulley and K. Weber, "Use of a horizontal ball mill to remediate per- and polyfluoroalkyl substances in Soil," *Science of The Total Environment*, vol. 835, p. 155506, 2022.
- [88] K. Aleksandrov, H.-J. Gehrman, M. Hauser, H. Mätzing, D. Pigeon, D. Stapf and M. Wexler, "Waste incineration of polytetrafluoroethylene (PTFE) to evaluate potential formation of per- and poly-fluorinated alkyl substances (PFAS) in flue gas," *Chemosphere*, vol. 226, pp. 898-906, 2019.
- [89] J. Maric, T. B. Vilches, S. Pissot, I. C. Vela, M. Gyllenhammar and M. Seemann, "Emissions of dioxins and furans during steam gasification of Automotive Shredder residue; experiences from the Chalmers 2–4-MW indirect gasifier," *Waste Management*, vol. 102, pp. 114-121, 2020.
- [90] N. R. Council, Review and evaluation of Alternative Chemical Disposal Technologies, Washington, D.C.: National Academy Press, 1996.
- [91] T. Ohlemiller, "Modeling of smoldering combustion propagation," *Progress in Energy and Combustion Science*, vol. 11, no. 4, pp. 277-310, 1985.
- [92] T. L. Rashwan, J. Gerhard and G. P. Grant, "Application of self-sustaining smouldering combustion for the destruction of wastewater biosolids," *Waste Management*, vol. 50, pp. 201-212, 2016.
- [93] A. L. Duchesne, J. Brown, D. Patch, M. D. W., K. P. Weber and I. J. Gerhard, "Remediation of PFAS-Contaminated Soil and Granular Activated Carbon by Smouldering Combustion," *Environmental Science & Technology*, 2020.
- [94] S. S. Toor, L. Rosebdahl and A. Rudolf, "Hydrothermal liquefaction of biomass: A review of Subcritical Water Technologies," *Energy*, vol. 36, no. 5, pp. 2328-2342, 2011.
- [95] J. Yu, A. Nickerson, Y. Li, Y. Fang and J. T. Srathmann, "Fate of per- and polyfluoroalkyl substances (PFAS) during hydrothermal liquefaction of municipal wastewater treatment sludge," *Environmental Science: Water Research & Technology*, vol. 6, no. 5, pp. 1388-1399, 2020.

- [96] G. L. Stegemeir and H. J. Vinegar, "Thermal Conduction Heating for In-Situ Thermal Desorption of Soils," in *Hazardous and Radioactive Waste Treatment Technologies Handbook*, 2001, pp. 1-37.
- [97] M. Söregård, A.-S. Lindh and L. Ahrens, "Thermal desorption as a high removal remediation technique for soils contaminated with per- and polyfluoroalkyl substances (PFASs)," *PLoS ONE*, vol. 15, no. 6, 2020.
- [98] M. Brusseau, H. R. Anderson and B. Guo, "Pfas concentrations in soils: Background levels versus contaminated sites," *Science of The Total Environment*, vol. 740, p. 140017, 2020.
- [99] Health Canada, "Guidelines for Canadian Drinking Water Quality: Guideline Technical Document — Perfluorooctanoic Acid (PFOA)," Water and Air Quality Bureau, Healthy Environments and Consumer Safety Branch, Health Canada, Ottawa, Ontario. (Catalogue No. H144-13/8-2018E-PDF), 2018.
- [100] A. Cordner, V. Y. De La Rosa, L. A. Schaider, R. A. Rudel, L. Richer and P. Brown, "Correction: Guideline levels for PFOA and PFOS in drinking water: The role of scientific uncertainty, risk assessment decisions, and social factors," *Journal of Exposure Science & Environmental Epidemiology*, vol. 29, no. 6, p. 157–171, 8 January 2018.
- [101] C. Wu, M. J. Klemes, B. Trag, W. R. Ditchte and D. E. Helbling, "Exploring the factors that influence the adsorption of anionic PFAS on conventional and emerging adsorbents in aquatic matrices," *Water Research*, vol. 182, p. 115950, 2020.
- [102] D. zhang, Q. He, M. Wang, W. Zhang and Y. Liang, "Sorption of perfluoroalkylated substances (pfass) onto granular activated carbon and biochar," *Environmental Technology*, vol. 42, no. 12, pp. 1789-109, 2019.
- [103] S. Barisci and R. Suri, "Occurrence and removal of poly/perfluoroalkyl substances (PFAS) in municipal and industrial wastewater treatment plants," *Water Science and Technology*, vol. 84, no. 12, pp. 3442-3468, 2021.
- [104] B. Göckener, A. Fliender, H. Rüdell, I. Fettig and J. Koschorreck, "Exploring unknown per- and polyfluoroalkyl substances in the German environment – the total oxidizable precursor assay as helpful tool in research and regulation," *Science of The Total Environment*, vol. 782, p. 146825, 15 August 2021.
- [105] R. Renner, "The long and the short of perfluorinated replacements," *Environmental Science & Technology*, vol. 40, no. 1, pp. 12-13, 2006.
- [106] E. Gagliano, M. Sgroi, P. Falciglia, F. Vagliasindi and P. Roccaro, "Removal of poly- and perfluoroalkyl substances (PFAS) from water by adsorption: Role of pfas chain length, effect of organic matter and challenges in adsorbent regeneration," *Water Research*, vol. 171, p. 115381, 2020.
- [107] J. Krug, P. M. Lemieux, C.-W. Lee, J. V. Ryan, P. Kariher, E. Shield, L. Wickersham, M. Denison, K. Davis, D. Swensen, R. Burnette, J. O. Wendt and W. Linak, "Combustion of C1 and C2 PFAS: Kinetic

Modeling and Experiments," in *Paper #IT3-04; Presented at 38th International Conference on Thermal Treatment Technologies and Hazardous Waste Combustors*, Virtual Meeting, 2021.

- [108] P. Glarborg, J. Miller, B. Ruscic and S. Klippentein, "Modeling Nitrogen Chemistry in Combustion," *Progress in Energy and Combustion Science*, vol. 67, pp. 31-68, 2018.
- [109] X. Yu, Y. Takabe, Yamamoto, C. Matsumura and F. Nishimura, "Biodegradation property of 8: 2 fluorotelomer alcohol (8: 2 FTOH) under aerobic/anoxic/anaerobic conditions," *Journal of Water and Environmental Technology*, vol. 14, no. 3, pp. 177-190, 2016.

Appendices

Appendix A: Pictures of the Laboratory Setup



Figure A.1: Cylinder unit holding PFAS-contaminated sand, with PFAS emission line, air line, and thermocouples connected to the top plate. Clay insulation was used to minimize the leakage.

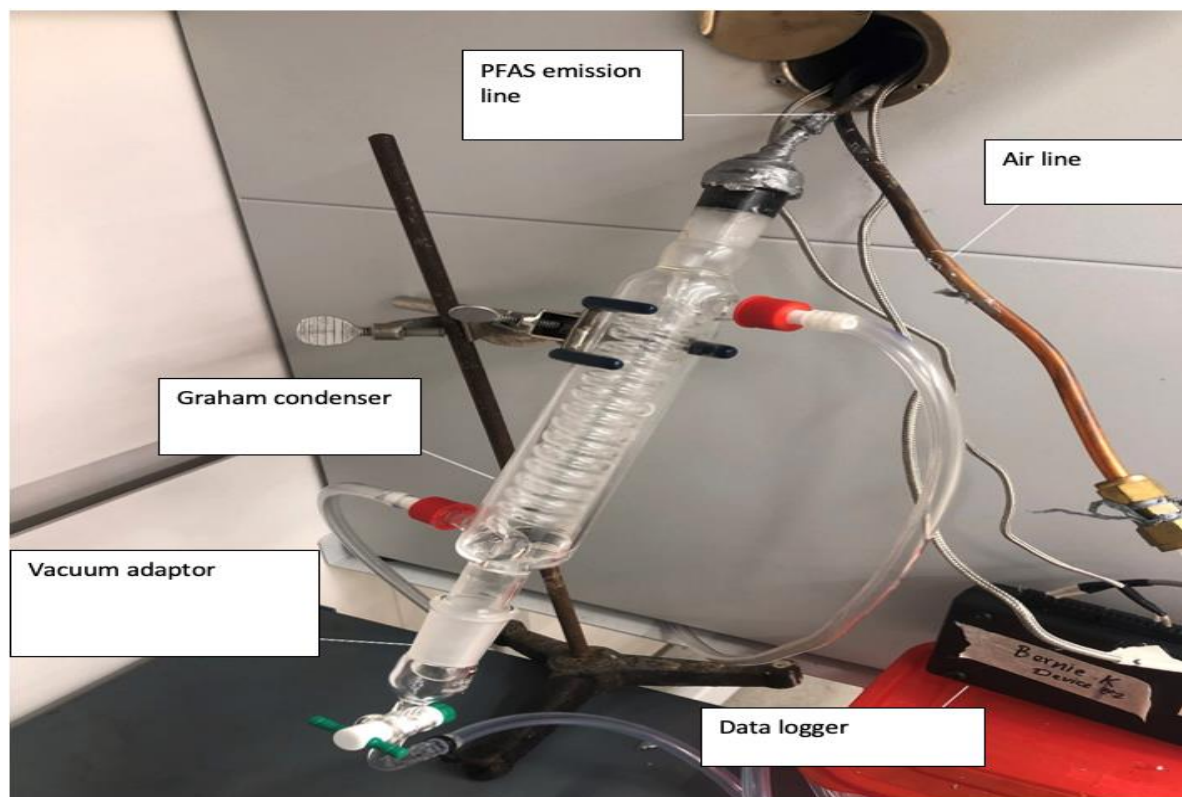


Figure A.2: First section of the PFAS emission system. The emission line extends from the opening at the side oven into a Liebig condenser. An air line passes through the opening into the cylinder, providing air to the cylinder holding PFAS-contaminated sand.

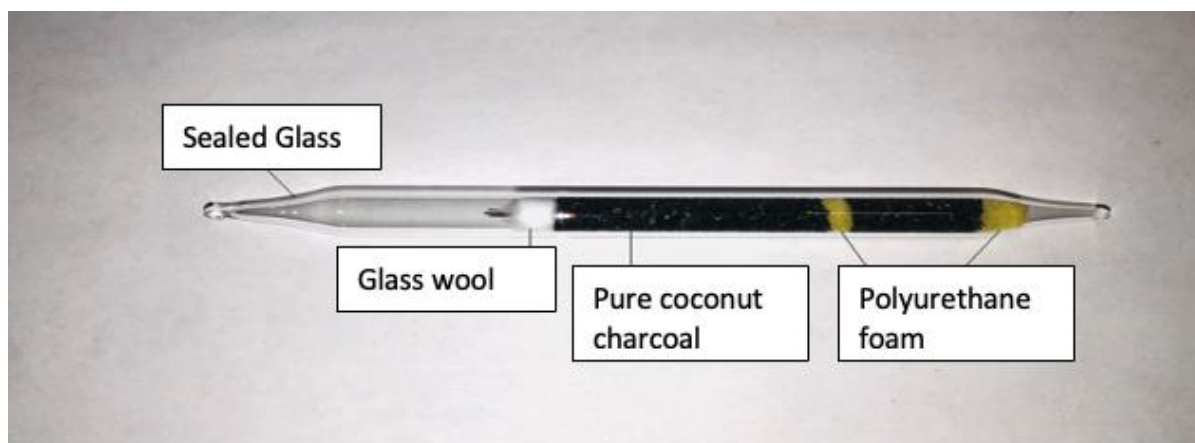


Figure A.3: Sorbent tube containing pure coconut shell charcoal 20/40 mesh thermally activated at 600 °C with polyurethane foam and glass wool sealed in glass.

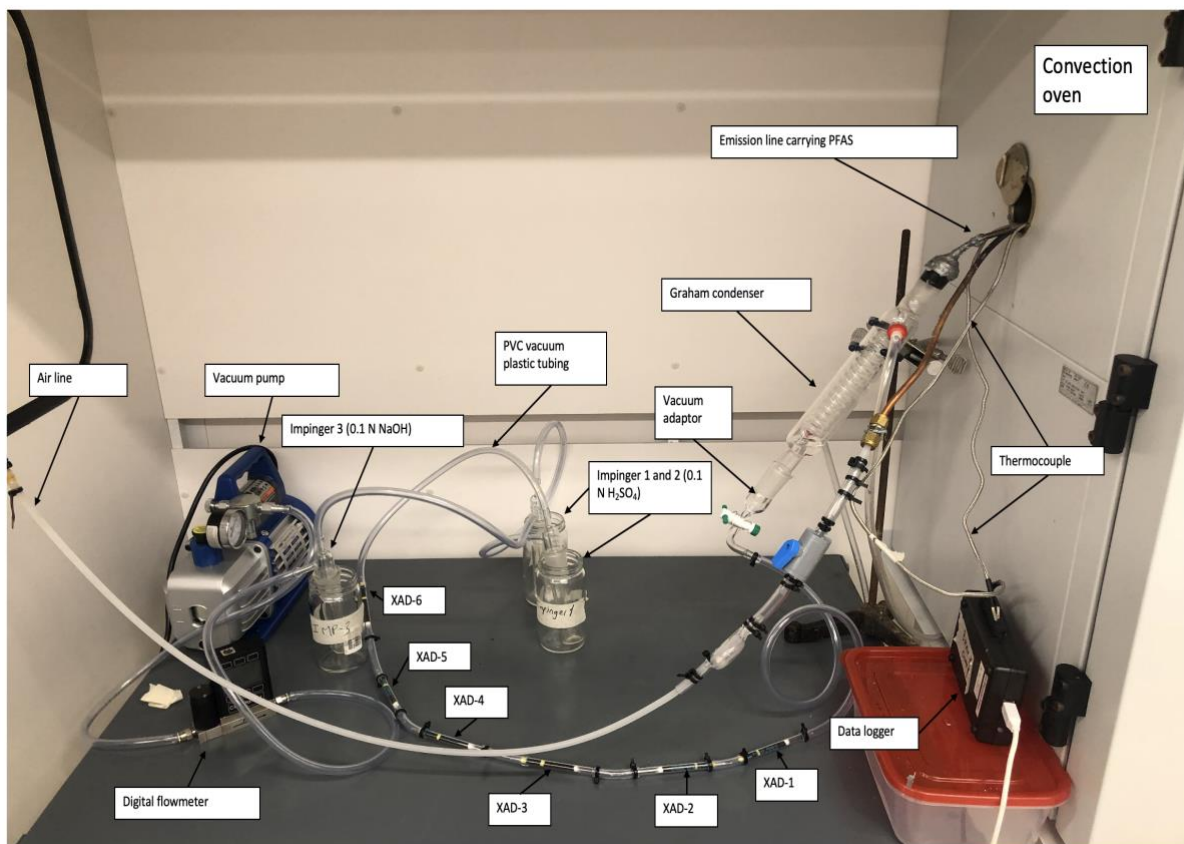


Figure A. 4: Experimental setup showing the PFAS emission system outside the oven.

Appendix B: PFAS Cylinder Setup and Temperature Profiles

One custom-made 1 L cylinder was fabricated to hold sand during the heating experiment. The cylinder was made of a 10.2 cm inner diameter and 13.2 cm long stainless-steel tube with two removable end plates secured using stainless steel quick clamps and high-temperature vermiculite gaskets (McMaster Carr #1089N18). The cylinder had four connections in the top plate, two were used to connect thermocouples, one was connected to an external air line that supplied air to the cylinder using a mass flow controller (FMA-1608A, Omega Ltd.), and one connected to a 0.25-inch outer diameter copper outlet tube to capture emissions.

Compression fittings (Swagelok SS-400-2BT) were used to secure all connections. Two (K-Type) high-temperature lead wire rugged thermocouples (Omega TJ36-CASS-14U-6-CC-XCIB) were fitted into the cylinder, allowing for temporal and spatial measurements for each experiment. The first thermocouple labeled “center” was inserted in the center of the top plate and extended 9 cm into the cylinder (almost at the center of the packed sand). The second thermocouple labeled “edge” was inserted at the midpoint between the center and the cylinder's edge and extended 9 cm into the cylinder. Thermocouple measurements were recorded in 3-second intervals using a data logger (DT9805, Data Translation Inc., Marlborough, MA).

The cylinder was filled with PFOA and PFOS-contaminated dry silica sand (AGSCO Corporation, 40/70, density = 2.65 g.cm⁻³). Once the sand was packed in place, a stainless-steel mesh (70 x 70 mesh size, 0.17 mm) with two holes for thermocouple access was placed on top of the dry sand. The mesh was used to prevent the rearrangement of the sand grains while the air was supplied, which would potentially cause clogging of the copper tube by sand particles. Each cylinder was weighed before and after loading with sand to ensure that the amount of sand added was accurate for mass balance purposes.

The cylinder was heated up in a convection oven (Carbolite Gero). The cylinder was connected to a copper tube threaded through an opening on the side of the oven, acting as an outlet for the volatile gas produced in the cylinder during heating. The gases inside the copper tubes leaving the oven were monitored using T-type thermocouples. The copper tube from the cylinder was connected to a Graham condenser (Cole-Parmer CNG200) using a rubber stopper. The condenser was used to reduce the temperature of the volatile gas to provide the ideal operating conditions for the XAD system. Cooled vapors from the Graham condenser were routed through a vacuum adaptor into a PFAS emission collection.

Three representative samples of the pre-treatment contaminated sand were collected for analysis for each experiment. The oven was preheated until it reached the desired temperature. The oven door was then opened slowly to prevent rapid temperature drops, and the cylinder was connected to the emission air line via fittings. A set air flux was introduced through the air line at the top of the cylinder using a mass flow controller (FMA-1608, Omega Ltd). Once the temperature of the sand covering both thermocouples and the gas leaving the emission line reached the targeted temperature, the vacuum pump was turned on. The average peak temperature for each experiment was monitored by a data logger (DT9805, Data Translation Inc., Marlborough, MA). Figure B. 1 shows the heating of the sand for the experiment at 550 °C. Channels (Ain-1) and (Ain-3) show the temperature of the sand inside the cylinder. Channel (Ain-4) shows the temperature of the gas leaving the cylinder into the emission line. Approximately 4 hours and 28 minutes were required for the sand to reach 550 °C, and an extra 30 minutes for the emissions released. Sand samples were collected in triplicate, analyzed, and averaged for each experiment. Even though the temperature of the sand was the same at the walls and edge of the cylinder, samples were collected from the center of the treatment zone at different elevations to capture all the PFAS present at different heights in the cylinder and avoid any heat losses at the walls of the cylinder.

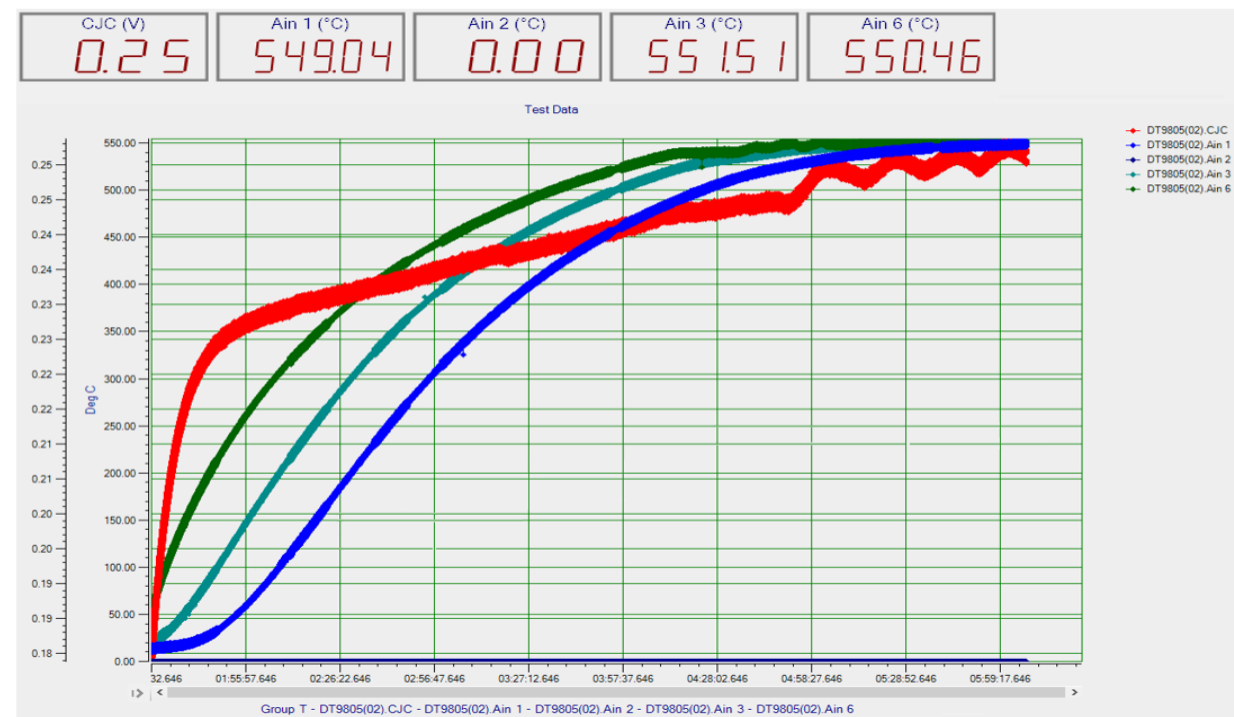


Figure B. 1: Temperature of heated sand at different thermocouple locations inside the cylinder

Appendix C: PFAS Analysis Procedure

C.1 Solid Sample Extraction

Sand samples were extracted by adding 10 mL of basic (1% ammonium hydroxide w/w) high-performance liquid chromatography (HPLC) grade methanol (CAS 67-56-1) to 1 gram of sand in a 15 mL c-tube. For the GACs, the entire tube was opened and added into 15 mL c-tubes, to which 10 mL of basic methanol was added. Some protocol adjustments were made by adding all the content of the sorbent tube, including glass wool, glass fiber filter, and polyurethane foam, into the 15 mL c-tubes. The samples were vortexed for 45 seconds and placed on an end-over-end shaker rotating at 70 rpm for 48 hours. The supernatant was filtered through a Whatman 0.45 mm glass microfiber filter into a 15 mL centrifuge tube at 4000 rpm for 15 minutes. A 1000 μ l subsample was placed into an HPLC vial for analysis. Any sample above 200 μ g/kg was diluted with basic methanol to below 200 μ g/kg. Liquid samples were directly sub-sampled into an HPLC vial for analysis.

Additionally, one of every ten samples was spiked with mass-labeled surrogates before extraction to track extraction efficiency. Every tenth vial was spiked with 100 μ L of PFDoA as an internal standard to track HPLC-mass spectrometer (MS) drift. Concentrations were not corrected based on mass-labeled surrogates, as recoveries were between 97–103% in all cases. Laboratory solvents were purchased from Fisher Scientific.

C.2 PFAS Targeted Analysis

Calibration standards for 13 compounds were analyzed. PFBA, PFBS, PFDA, PFDoA, PFHpA, PFHxA, PFHxS, PFNA, PFOA, PFOS, PFOSA, PFPeA and PFUnA were prepared using basic methanol from solid reagents at a range of 0.1 to 250 ppb. Continuing calibration verification

(CCV) was performed at the beginning and end of each experiment at 0.4 ppb to 100 ppb. These CCV samples were prepared using high purity liquid standards.

Liquid chromatography was performed on an Agilent 1260 Infinity Series Bio-Inert HPLC system implementing two mobile phases. The first was HPLC-grade water with ammonium acetate (2 mM). The second was methanol with ammonium acetate (2 mM). The gradient was delivered at a 0.4 mL/min flow rate and a 10 μ L injection volume. A Zorbax Eclipse Plus C18 Column was implemented simultaneously with a paired guard column. Initial eluent conditions were 94% water and 6% methanol. The methanol percentage was increased to 100% over six minutes, held at 100% methanol for eight minutes, and then decreased for 11 minutes. The column was then allowed to re-equilibrate to the initial eluent concentration for four minutes before the subsequent sample analysis.

An Agilent 6460 Triple Quadrupole Mass Spectrometer LC-MS/MS operating in negative electrospray ionization mode running in MRM mode was used for sample analysis. Two MRM transitions were included for all analytes, but some analytes only had a single transition available. Each transition had a dwell time of 120 ms. The transitions were analyte-dependent and the same as those used previously for the mentioned suite of 13 PFAS.

The instrument operated at the optimal source parameters: voltage, 4,000*V; curtain gas flow, 35 arbitrary units (au); nebulizer gas flow, 50 au; turbo gas flow, 50 au; medium collision gas flow; and source temperature, 650 °C. Nitrogen was supplied from a NitroFlow gas generating system and was used for the drier and nebulizer gas, and a nitrogen tank was used as the curtain and collision gas. Quantification was performed using Masshunter Quantification Software with a calibration curve with an R^2 value greater than 0.99. The quantitation limits were analyte, matrix, and run-dependent but were approximately 1 ng/g in the sand and 0.4 ng/mL in aqueous samples.

Limits of detection were also analyte, matrix, and run-dependent but were about 0.1 ng/g in the sand and 0.01 ng/mL in aqueous samples.

C.3 PFAS Suspect Screening Analysis

It is important to acknowledge that the mass spectrometer used for this suspect screening analysis is not made for this purpose. It does not have the resolution to allow high confidence mass target matching. Using a liquid chromatography high-resolution mass spectrometer (LC-HRMS) would have benefited this study. This suspect screening was only used to measure semi-qualitative data. Suspect screening analysis was performed high to try and quantify the possible formation of by-products that have been observed in various remediation studies. The objective was to watch larger-chained PFAS transformation (PFOA, PFOS) into shorter-chain carboxylates. A list of compounds was compiled from the literature. This list consists of TFA, PFPA, PFBA, 6:2 FTCA, and single H/F-exchanged carboxylate PFAS.

The suspect screening was performed on the same instrument set-up used for targeted analysis, except a 150 mm analytical column was used to improve analyte separation. For suspect screening analysis, 10 methanol blanks were injected into the system to eliminate any background contamination. A solvent blank, reagent blank, method blank, pre-contaminated sand, clean GAC sample, and emission-capture GAC samples were analyzed sequentially using a mass scan mode. The emission-capture GAC samples had masses not found in any pretreated sand samples, indicating some PFAS transformation products. The masses obtained from the emission-capture GAC sample were compared to the suspect compound list, with many masses matching those of suspect compounds.

C.4 Fluoride ion-selective electrode (ISE)

One gram of sand was weighed into a 15 mL centrifuge tube, and 4 ml of DI water was added. The sample was placed on a shaker for 48 hours at 170 rpm and then centrifuged at 4000 rpm for 20 minutes. Two ml of the supernatant was transferred into a 15 mL centrifuge tube, and 1 mL of the TISAB (Fisher Scientific) was added. A calibrated Fisher Scientific Orion ISE was placed into the sample, and measurements were recorded when the reading was stabilized. The detection and quantification limits were approximately 1 ppm and 0.5 ppm, respectively. The method was modified from EPA Method 9214.

Appendix D: Quality Control and Quality Assurance Guidelines

Sample triplicate results consistent with a relative percent deviation of less than 30% were considered acceptable. All method blanks, reagent blanks, and instrument blanks were below the quantification limit for the methods used. Instrument duplicates analyzed at the start and end of each sample run were within acceptable guidelines (<30% deviation). Mass-labeled surrogate recovery for sand extraction methods was adequate (between 70–130%). Internal standards (IS) used to track instrument drift was permissible (<30% instrument response drift over the analysis period, confirmed through both instrument duplicates and IS tracking).

Appendix E: Experimental Cleaning Procedure

All Samples bottles, glassware, and cylinder for the four experiments were rinsed three times with deionized water, followed by three rinses with methanol (CAS 67-56-1) and three times with isopropyl alcohol (CAS 67-63-0). All copper tubing and PVC tubing were replaced for each experiment. The cleaning protocol was adjusted to ensure no contamination between experiments and when collecting samples.

Appendix F: PFOA and PFOS Pre- and Post-treatment Concentrations

Table F. 1: PFAS in Pre- and Post-Treatment Media (ppm) at 550°C, 500°C, and 400°C

PFAS name	PFAS-spiked sand (mg/kg)	Post-treatment 550 °C	Post-treatment 500 °C	Post-treatment 400 °C
PFOA-C ₈	112.570± 9.00 ^b	B.D.L ^a	0.080	0.030
PFOS-C ₈	129.011 ± 10.32 ^b	0.020	0.080	B.D.L ^a
PFHxDA-C ₁₁	0.0100	B.D.L	0	B.D.L ^a

^aB.D.L = 0.0003 mg/kg

^bUncertainty of the pre-treatment PFAS₁₃ were calculated using the 95% confidence interval of the concentration measured by the analytical method.

Table F. 2: PFAS in Pre- and Post-Treatment Media (ppm) at 300°C and 250°C

PFAS name	PFAS-spiked sand (mg/kg)	Post-treatment 300 °C	Post-treatment 250 °C
TFA-C ₂	B.D.L	0.011	0.010
PFPA-C ₃	B.D.L	0.975	0.010
PFBA-C ₄	B.D.L	1.866	0.020
PFPeA-C ₅	B.D.L	0.071	0.100
PFHxA-C ₆	B.D.L	0.141	0.560
PFHpA-C ₇	B.D.L	0.196	1.651
PFOA-C ₈	25.655±2.25 ^b	0.220	3.250
PFOS-C ₈	25.960±2.07 ^b	3.815	4.991
PFOSA-C ₈	B.D.L	B.D.L	0.010
6-2FTSA-C ₈	B.D.L	B.D.L ^a	0.010
PFNA-C ₉	B.D.L	B.D.L	0.010
PFDA-C ₁₀	B.D.L	B.D.L	0.010
PFUnDA-C ₁₁	2.9	0.010	0.010

^aB.D.L = 0.0002 mg PFAS/kg solid.

^bUncertainty of the pre-treatment PFAS₁₈ were calculated using the 95% confidence interval of the concentration measured by the analytical method.

Appendix G: Mass of Fluorine Recovered from Each Experiment

Table G. 1: Estimated Fluorine Mass (μg) in Sand and Emission at 550°C, 500°C, 400°C, 300°C, and 250°C only accounting for 5% of the emission that are being captured

Temperature	Pre-treatment porous media (ug F)	Post-Treatment PFAS in Sand (ug F)	PFAS in Emission System (ug F)	Fluoride ion Post-treated Sand (F-)	Fluoride Ion Impingers (F-)
250°C	39722.064	7002.096	118.377	293.797	3.081
300°C	31448.776	3641.890	164.958	406.854	19.429
400°C	32196.550	3.765	749.527	289.381	3.482
500°C	32196.550	20.857	997.520	452.220	3.399
550°C	32196.550	17.882	1875.819	373.081	3.346

Appendix H: Mass of Individual PFAS captured by the Emissions

Table H. 1: Mass(μg) of the individual PFAS18 captured by the emission

PFAS Name	PFAS on emission (μg)				
	250°C	300°C	400°C	500°C	550°C
TFA-C ₂	0.449	1.546	B.D.L	323.818	1099.829
PFPA-C ₃	0.636	2.297	2.897	23.202	616.212
PFBA-C ₄	1.387	4.167	5.295	17.010	16.482
PFBS-C ₄	B.D.L	B.D.L	B.D.L	B.D.L	B.D.L
PFPeA-C ₅	3.276	11.587	10.722	26.860	14.444
PFHxA-C ₆	9.315	22.864	21.777	39.675	22.395
PFHxS-C ₆	B.D.L	B.D.L	B.D.L	B.D.L	B.D.L
PFHpA-C ₇	16.083	31.123	56.949	67.027	37.634
PFHpS-C ₈	B.D.L	B.D.L	B.D.L	2.367	1.031
PFOA-C ₈	140.191	128.166	976.052	977.379	1437.979
PFOS-C ₈	0.203	205.837	17.647	81.222	128.845
PFOSA-C ₈	0.049	B.D.L	B.D.L	B.D.L	0.284
6:2 FTS-C ₈	0.004	0.010	B.D.L	B.D.L	B.D.L
PFNA-C ₉	0.086	0.019	0.013	1.454	1.391
PFDA-C ₁₀	0.868	0.408	1.016	1.611	3.033
PFUnDA-C ₁₁	0.317	0.381	B.D.L	0.301	0.653
PFDoDA-C ₁₂	B.D.L	B.D.L	B.D.L	0.131	0.49
PFDoS-C ₁₂	B.D.L	0.003	B.D.L	B.D.L	B.D.L
PFTrDA-C ₁₃	B.D.L	B.D.L	B.D.L	0.062	0.344
PFTDA-C ₁₄	B.D.L	B.D.L	B.D.L	0.021	0.174
PFHxDA-C ₁₆	B.D.L	B.D.L	B.D.L	B.D.L	B.D.L
PFODA-C ₁₈	B.D.L	B.D.L	B.D.L	B.D.L	B.D.L

Appendix I: List of Known PFAS Detected in the First sorption Tubes at 550°C

Table I. 1: Concentration of PFAS detected in the first sorption tube at 550 °C

Abbreviation	XAD-1 (mg/kg)
TFA-C ₂	541.281
PFPA-C ₃	55.422
PFBA-C ₄	12.184
PFPeA-C ₅	15.723
PFHxA-C ₆	22.663
PFHpA-C ₇	34.618
PFOA-C ₈	932.481
PFOS-C ₈	1.030
PFNA-C ₉	1.632
PFDA-C ₁₀	2.791
PFUnDA-C ₁₁	0.774
PFDoDA-C ₁₂	0.583
PFTTrDA-C ₁₃	0.412
PFTDA-C ₁₄	0.210

Appendix J: Orbitrap Experimental Setup

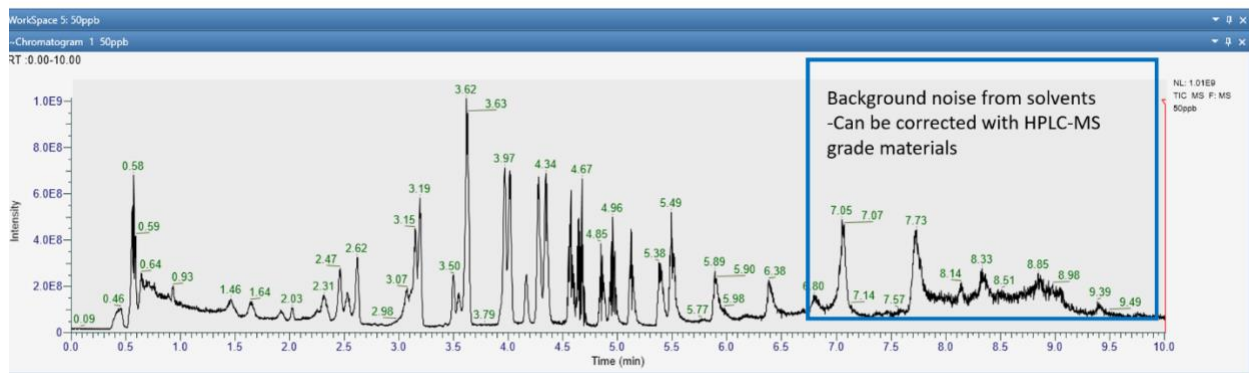


Figure J. 1 : 50 ppb standard for the first XAD showing the background noise far delayed in the column

A Thermofisher Orbitrap Exploris 120 was used to discriminate ions of interest from interfering ions differing by only very small mass increments at a mass-to-charge ratio as low as 40 m/z . The Orbitrap was coupled to an ACME C-18 plus column to reach high pressure and physical separation that helps target unique elution conditions. Shorter chain PFAS will elute first, and in terms of functional groups, the carboxylates will elute, followed by sulfonates and sulfonamides. For example, PFOA will elute in 6.38 minutes, PFOS in 4.3 minutes, PFODA or the C-18 carboxylate in 6.38 minutes, and PFOSA in 7.03 minutes. So, when looking at the C-18 carbon length vs. C-8, the sulfonamide dominates for the retention time of the column. The system's pH was 4, which caused the PFOSA ending column to be neutrally charged, which is why it is retained on the column quite easily. PFOSA is neutral compared to everything else negatively charged; therefore, it moved through the water much more quickly.

The Orbitrap was flushed for an hour to remove the background noise and organic impurities, followed by 10 blanks. A fresh blank was eluted five times to establish the baseline signal and run the calibration sample to establish the retention time and instrument accuracy. Finally, the experimental sample was analyzed. The software was then provided with the specific elements to examine in the AI-based mathematical molecule fitting. The machine was set to look for carbon,

oxygen, hydrogen, sulfur, fluorine, and nitrogen. The fitting software then used a series of matrices to establish the best fit to select the least likely molecule while performing the scan. The interpretation provided by the software is based on the knowledge of the system and the chemistry as understood by the operator. For example, PFOS ($C_8O_3F_{17}S$) has a combined score of 98.34, and its closest competitor is $C_8O_6N_2F_{13}S$, a virtually impossible formula. Additional information such as fragmentation patterns and similar molecule retention times were used to reinform the molecular knowledge. After flushing the system and running the calibration sample, some background noise must be accounted for as the experiments proceed. This noise can be corrected using HPLC-MS grade material. Finally, while the 50-ppb standard was running, most of the background noise and impurities were far delayed in the column, and most of the standards appeared well before that peak.

Appendix L: List of Unknown PFAS Detected in the First sorption Tubes at 550°C

Table L. 1: List of PFAS compounds detected solely based on the visual identification of the peaks of the orbitrap XAD-1 at 550°C

Retention Time (minutes)	Peak Mass (g/mole)	Likely Compound (-H)	Peak Area	Note
3.6	412.965	PFOA (C8O2F15)	2.00E+09	
6.5	411.981	C ₈ HONF ₁₅	3.80E+08	PFAS Amide (C4-C17 found)
3.4	336.972	C ₈ O ₂ F ₁₁	3.00E+08	Double Alkene PFOA
2.6	339.017	C ₁₀ H ₄ ON ₂ F ₉	2.70E+08	
3.29	371.991	C ₁₀ H ₃ O ₄ NF ₉	2.60E+08	
3.1	419.984	C ₁₀ HO ₃ N ₃ F ₁₁	2.20E+08	
3.3	469.980	C ₁₁ HO ₃ N ₃ F ₁₃	2.00E+08	
5.75	360.027	C ₁₀ H ₇ O ₃ NF ₉	1.60E+08	
5.4	359.044	C ₁₀ H ₈ O ₂ N ₂ F ₉	1.00E+08	
5	344.044	C ₉ H ₇ ON ₃ F ₉	6.00E+07	
2.63	369.987	C ₉ HO ₃ N ₃ F ₉	6.00E+07	
4.5	436.040	C ₁₆ H ₈ O ₂ NF ₁₀	5.00E+07	
6	361.985	C ₇ HONF ₁₃	3.70E+07	PFAS Amide
6.4	352.994	C ₈ HN ₂ F ₁₂	3.50E+07	PFAS Amine?
6.35	415.995	C ₁₀ H ₃ O ₂ NF ₁₃	3.00E+07	
3.56	394.975	C ₈ HO ₂ F ₁₄	3.00E+07	-F/+H Exchanged PFOA
4.5	594.962	C ₁₂ HO ₂ F ₂₂	2.00E+07	
5.5	311.988	C ₆ HONF ₁₁	1.00E+07	PFAS Amide
6.8	485.998	C ₁₁ H ₄ O ₂ NF ₁₆	1.00E+07	
4.83	218.999	C ₅ HON ₂ F ₆	6.00E+06	

4.83	261.991	C ₅ HONF ₉	9.00E+05	PFAS Amide
3.92	211.995	C ₄ HONF ₇	9.00E+05	PFAS Amide
2.64	161.998	C ₃ HONF ₅	2.00E+05	PFAS Amide